Journal of Medicinal Chemistry

Article

2,4,6-Substituted Quinazolines With Extraordinary Inhibitory Potency Toward ABCG2

Michael K Krapf, Jennifer Gallus, Vigneshwaran Namasivayam, and Michael Wiese

J. Med. Chem., **Just Accepted Manuscript** • DOI: 10.1021/acs.jmedchem.8b01011 • Publication Date (Web): 03 Aug 2018

ACS Publications

is published by the American Chemical Society. 1155 Sixteenth Street N.W., Washington, DC 20036

Abstract

Several members of the ABC transporter superfamily play a decisive role in the development of multidrug resistance (MDR) in cancer. One of these MDR associated efflux transporters is ABCG2. One way to overcome this MDR is the co-administration of potent inhibitors of ABCG2.

In this study we identified novel inhibitors containing a 2,4,6-substituted quinazoline scaffold. Introduction of a 6-nitro function led to extraordinarily potent compounds, that were highly selective for ABCG2 and also able to reverse the MDR toward the chemotherapeutic drugs SN-38 and mitoxantrone. The binding of substrate Hoechst 33342 and the two potent inhibitors **31** and **41** which differ in their mechanism of inhibition was rationalized using the recently published cryo-EM structures of ABCG2. For a better understanding of the interaction between the inhibitors and ABCG2, additional investigations regarding the ATPase activity, the interaction with Hoechst 33342 and with the conformational sensitive 5D3 antibody were carried out.

Introduction

ATP-binding cassette transport proteins are widely expressed in different tissues where they perform the efflux of structurally diverse substrates out of the cells. The excretion is powered by ATP hydrolysis, forming ADP and inorganic phosphate, and occurs even against a concentration gradient.[1] In humans 48 ABC transport proteins are expressed which can be classified according to their phylogenetic similarity in seven subfamilies labelled ABC A to ABC G.[2, 3, 4, 5] ABC transport proteins are often expressed in tissues with a barrier function, where they protect the cells from harmful substances, but can also effectuate the membrane transport of nutrient.[6] Unfortunately, many cytostatic drugs are substrates of ABC transporters and their overexpression in cancer cells persists as a major obstacle in the chemotherapeutic treatment.[7] This so-called multidrug resistance (MDR) is mainly related to the expression of the three major MDR-associated transport proteins P-glycoprotein (P-gp, ABCB1), multidrug-resistance associated protein 1 (MRP1, ABCC1) and breast cancer resistance protein (BCRP, ABCG2).[8,9,10] ABCG2 was discovered last when the workgroup of Doyle *et al.* identified the transport protein in a human breast cancer cell line, which was selected for doxorubicin resistance in the presence of verapamil, an inhibitor of P-gp.[11,12,13] High levels of ABCG2 are often found in tissues performing a protective function or tissues which are associated with the homeostasis of nutrients and hormone.[14] Interestingly, the structure of ABCG2 differs from ABCB1 and ABCC1: being a half transporter, ABCG2 is assumed to form dimers or tetramers for function while ABCB1 and ABCC1 are expressed in their fully functional form.[15, 16, 17, 18] ABCG2 is composed of 655 amino acids and consists of only one cytosolic nucleotide-binding domain (NBD) and one transmembrane domain (TMD).[19] To date the function of ABCG2 remains unclear and further investigations are important to effectively treat ABCG2 overexpressing cancers.[20,21,22] As mentioned before, a common problem in the chemotherapeutic treatment of cancers is that many cytostatic drugs are substrates of ABC-transport proteins like ABCG2: the anthracene derivative mitoxantrone (MX) for instance is a

substrate of ABCG2 and can be used to select cells with an overexpression of ABCG2, based on the resistance toward the cytostatic drug.[23,24] Another substrate of ABCG2 is the cytostatic drug SN-38, which is an active metabolite of irinotecan.[25,26] Both, MX and SN-38, have already been used in our prior studies to investigate the reversal of the MDR in MDCK II BCRP cells by co-administering inhibitors of ABCG2.[27]

Although co-administration of potent inhibitors is one way to overcome MDR, the scientific community has become more cautious in terms of *in vivo* application of inhibitors of ABCG2, since the promising *in vitro* results with inhibitors of ABCB1 led to disappointing outcomes in the clinic. Nevertheless, several studies found a correlation between the overexpression of ABCG2 and a worse clinical outcome, while other studies remain sceptical toward that topic.[28,29,30]

The first potent inhibitor of ABCG2 was isolated from *Aspergillus fumigatus* and named fumitremorgin C. Despite its high inhibitory potency the high neurotoxic effects prevented any clinical use.[31] The second generation inhibitor **59** was more promising, since it exhibited less toxic effects, a high selectivity toward ABCG2 up to 1 μM and an considerably high inhibitory potency.[32,33] Its application in photodynamic therapy for instance has already led to promising results, where the efflux of phototoxic agents could be inhibited by co-administration of compound **59** and resulted in a higher effectiveness of the therapy.[29,34] Other inhibitors have already been used in cancer therapy. For instance some compounds in the class of tyrosine kinase inhibitors (TKIs) were found to be useful drugs in chemotherapeutic treatment. Preliminary *in vitro* investigations of the workgroup of Ozvegy-Laczka *et. al.* found a high affinity interaction of several TKIs with ABCG2, some even at submicromolar concentration.[35,36] The TKI gefitinib for instance is currently used as a drug for certain breast, lung and other cancers. However, only very few selective and potent inhibitors of ABCG2 active at a submicromolar concentration have been reported.[37]

Our workgroup modified the basic quinazoline scaffold of gefitinib and carried out different modifications: in our previous studies we found that an aromatic residue at position 2 and a substituted aniline linker at position 4 led to a considerably higher inhibitory potency and selectivity toward ABCG2 compared to gefitinib.[27,56] We also identified some structural features that have an impact on the selectivity of a substance: in particular the presence of methoxy substituents was found to increase the inhibitory potency toward ABCB1 and also ABCC1. In contrast, potent and selective compounds often contained nitro functions at the aniline moiety at position 4 of the quinazoline scaffold.

In the current work, we started from our 2,4-disubstituted quinazoline scaffold and introduced nitro, amino and some other groups at position 6. These new derivatives were compared to some of our previous compounds providing new insights into the structure-activity relationship of these novel derivatives. Most notably, substitution with nitro at position 6 resulted in extraordinarily potent and selective inhibitors of ABCG2.

Results and Discussion

Chemistry.

The synthetic route for all compounds of this work is illustrated in Scheme 1. First, 2-amino-5-nitrobenzoic acid was reacted with phosgene to form a cyclic anhydride. Subsequently, the anhydride function underwent cleavage when bubbling gaseous ammonia through the reaction mixture to form 2-amino-5-nitrobenzamide **1**, the precursor for the following steps. The 2-phenylquinazolinone derivatives **2**-**7** were obtained by cyclisation of **1** with a substituted benzaldehyde. Substitution of the carbonyl function with chlorine was achieved by reaction with $POCl_3$ to yield the 4-chloroquinazoline derivatives **8**-**13**. A nucleophilic substitution of chlorine at position 4 was carried out with different aniline derivatives using microwave radiation to yield compounds **14**-**42**. Compound **20**, which contains a 3',4'-dimethoxy residue, was treated with boron tribromide to obtain a 3',4'-dihydroxy function at the aniline

linker (**16**). Moreover, the nitro function at position 6 was converted into an amino group. Therefor, a Pd/C catalysed hydrogenation was performed in a pressure vessel. The obtained 6-amino derivatives **43**-**47** were then reacted in a nucleophilic substitution with different acid chlorides to yield compounds **48**-**51**.

Based on our potent 2-phenyl-4-anilinoquinazoline derivatives, we carried out further modifications at position 2 and most notably at position 6. This idea was inspired by the fact that many inhibitors containing a quinazoline structure like gefitinib possess substitution at position 6 and sometimes also at position 7. Therefore, we introduced nitro, amino and aromatic functions at position 6 to elucidate the impact of these modifications on the inhibitory activity toward ABCG2. In general, we preferred substituents, such as cyano, nitro, fluoro and hydroxy, which exhibited high potencies at position 4 in our previous work.[27] There we found that high potencies were obtained in either *meta* or *para* position depending on the function introduced at the anilino moiety: functions with negative mesomeric effects were in most cases more beneficial in *para* position whereas substituents with positive mesomeric effects mostly led to high potencies in *meta* position. Thanks to a facile comparison with our compounds investigated in earlier studies, we were able to find structure-activity relations that could be beneficial for subsequent synthesis.

Identity of all compounds was confirmed by ^{1}H and ^{13}C NMR spectra and the purity by elemental analysis.

Biological evaluation.

Hoechst 33342 Accumulation Assay. The inhibitory potency of the test compounds toward ABCG2 was determined by the well-established Hoechst 33342 accumulation assay. The principle of the assay is based on the efflux of the fluorescent dye Hoechst 33342, a substrate of ABCG2, out of the cell. Hoechst 33342 only shows low fluorescence intensities in watery environment, but fluorescence increases considerably upon binding to DNA or embedding in

a lipophilic environment like a cell membrane.[38] Inhibition of the transport protein results in an increased intracellular accumulation of Hoechst 33342 that leads to higher fluorescence which can be correlated to the inhibitory potency of a compound. Structural formulas of Hoechst 33342 and the other substrates and standard inhibitors of ABCG2 are given in Figure 1 for reference.

Inhibitory activities of the test compounds **14-58** from the Hoechst 33342 accumulation assay are presented in Table 1. A quick overview illustrating the SAR of the investigated compounds is provided at the end of this chapter (Figure 2).

Compounds **14-42** all contain a nitro group at R^3. At first, the unsubstituted basic structure **14** with phenyl at R^1 and hydrogen at R^2 was investigated. Interestingly, the resulting IC_{50} value of 106 nM is considerably lower than its analogue **52** (IC_{50} = 882 nM) lacking the nitro function at R^3. Subsequently, polar groups were investigated at R^2 using a 3'-hydroxy (**15**) and 3',4'-dihydroxy (**16**) substitution, of which the mono-substitution yielded a low IC_{50} value of 65.3 nM and the disubstitution an IC_{50} value of 119 nM. Even higher activities resulted by a substitution with 3-methoxy (**17**) and 3',4'-dimethoxy (**18**) at R^2, with remarkably low IC_{50} values of 33.1 nM and 37.0 nM. In contrast, the well-known and highly potent standard inhibitor **59** yielded a higher IC_{50} of 227 nM. In comparison to the 3',4'-dimethoxy quinazoline analogue **53**, lacking the nitro function at R^3, compound **18** is about four-fold more potent. Derivatives with 3'-cyano (**19**) or 4'-cyano (**20**) at R^2 possessed IC_{50} values of 48.2 nM and 48.1 nM, respectively. The 2-phenylquinazoline analog **54**, which showed the highest activity in our earlier study yielded in a slightly higher IC_{50} of 69.9 nM. Similar activities resulted from a 3'-fluoro (**21**: 51.5 nM) and a 3'-trifluoromethyl (**22**: 49.1 nM) substituent. Again, the 3'-fluoro analogue **55**, lacking the nitro function at R^3, showed a considerably lower potency with an IC_{50} value of 355 nM. Also the 3'-nitro-4'-hydroxy (R^2) 6-nitro derivative **23** was more potent (IC_{50} = 37.4 nM) than its analogue **56** (IC_{50} = 80.0 nM). Also compound **24** containing an acetamido group (IC_{50} = 78.7 nM) was significantly more

potent than its analog **57** without 6-nitro group (IC_{50} = 278 nM). Surprisingly, compound **25** with a carboxyl residue led to an IC_{50} in the submicromolar range (904 nM), although it forms an anionic species under physiological conditions decreasing the membrane permeability of this derivative. Comparison with its analog **58** (IC_{50} = 6380 nM) once again illustrates the beneficial impact of the 6-nitro group.

For the next compounds, the phenyl residue at R^1 was replaced by a more hydrophilic pyridyl residue. First, a 3-pyridyl residue was combined with 3'-methoxy (**26**: IC_{50} = 47 nM) and 4'-methoxy (**27**: IC_{50} = 57.7 nM) at R^2, respectively. In comparison to compound **27** the 4-pyridyl analog **28** led to a comparable potency (IC_{50} = 75.5 nM). Also, the interchange of phenyl with pyridyl had no major impact on the IC_{50} value, illustrated in the compound pairs **17**/**26** and **19**/**29**.

In the next series a 3-trifluoromethylphenyl substituent was introduced at R^1. Interchange of the trifluoromethyl group between the aromatic cores at position 2 and 4 resulted in similar high potencies in the range of 50-60 nM (compare compounds **22** and **30**). Extraordinarily high inhibitory activities resulted from substitutions at R^2 with 3'-hydroxy (compound **31**, IC_{50} = 27.6 nM), 3',4'-dimethoxy (**33**, IC_{50} = 30.2 nM), 3'-fluoro (compound **35**, IC_{50} = 44.8 nM), 3'-nitro-4'-hydroxy (compound **38**, IC_{50} = 33.0 nM) and 3'-acetamido (compound **39**, IC_{50} = 44.8 nM). Substitution with 3'-methoxy or 3'-thiomethyl as well as 3'- or 4'-nitro resulted in good activities between 60 and 100 nM (compare compounds **32**, **34**, **36** and **37**). Except for compound **32** all 3-trifluoromethylphenyl derivatives possessed a similar or even higher potency than their corresponding phenyl analogs.

Additionally, two 3-methoxyphenyl (R^1) derivatives were synthesized containing a 4'-cyano (**40**) or 3'-fluoro substituent (**41**) at R^2. Surprisingly, both derivatives yielded very high inhibitory activities with IC_{50} values of 27.8 nM for compound **40** and 23.4 nM for **41**, which is the most potent compound in the test set. Compared to their phenyl analogs **20** and **21** they are roughly two-fold more potent, and compound **41** shows a nine-fold higher activity than

the standard inhibitor compound **59**. Concentration-response curves of **40**, **41** and **59** are depicted in Figure 3. Moreover, the 3,4-dimethoxyphenyl (R^1), 3'-trifluoromethyl at R^2 derivative **42** yielded an IC_{50} value of 57.2 nM. Unfortunately, the 3,4-dimethoxy substitution did not increase the potency in comparison to compound **22**, which contains a phenyl group at R^1 instead.

In the next series, the 6-nitro functions of some derivatives were reduced to an amino group. Free amino groups act as H-donor functions and increase the electron density at the attached aromatic cores, whereas nitro groups are H-acceptor functions and decrease the electron density.

First, a 3-pyridyl residue at R^1 was combined with either a 3'-methoxy (**43**) or a 4'-methoxy group (**44**) at R^2. The 3'-methoxy derivative yielded an IC_{50} value of 369 nM whereas the *para* substituted compound had a twofold higher IC_{50} value of 646 nM. Three more 6-amino derivatives were investigated containing a 3-trifluoromethylphenyl residue at R^1: compound **45** with a no substituent at R^2 possessed an IC_{50} of 726 nM, whereas substitution with 3'-hydroxy and 3'-methoxy resulted in IC_{50} values of 799 nM and 835 nM for compounds **46** and **47**, respectively. The comparison with their 6-nitro analogs illustrates that the amino function at position 6 lowers the inhibitory potency of all compounds to a considerable extent.

Subsequently, the amino function at R^3 was modified by introducing aromatic groups and one ester function. Initially, a substitution with 3-pyridyl at R^1, 3'-methoxy at R^2 together with *N*-1-iminoethyl acetate at R^3 was carried out for compound **48**. The resulting IC_{50} value of 5310 nM illustrates the strong loss of potency in comparison to compound **43** with the free amine at R^3. Also, substitution with *N*-3-nitrobenzamide (**49**: IC_{50} = 1150 nM) and *N*-nicotinamide (**51**: IC_{50} = 1040 nM) resulted in a decrease of inhibitory potency in comparison to compound **43**. Also the 4-methoxy (R^2) analog of compound **49**, namely compound **50**, yielded a far higher IC_{50} value of 1620 nM compared to its 3-methoxy counterpart.

In summary, the investigation of our new 2-substituted-4-anilinoquinazoline derivatives containing additional substitution at position 6 revealed several findings: Extraordinary high inhibitory activity toward ABCG2 resulted from nitro functions at R^3. Most notably, the presence of methoxy and hydroxy groups led to very high potencies, as observed for compounds **17**, **18**, **23**, **31**, **33**, **38**, **40** and **41**. The unsubstituted compound **14** showed a lower inhibitory activity than the substituted 6-nitro derivatives, which is in good accordance to our previous results for the 4-substituted-2-phenylquinazolines (compare compounds **52-58**). The most potent compound **41** containing a 3-methoxyphenyl group at R^1 and 3'-fluoro substituent at R^2 possessed a nearly ten-fold higher potency than compound **59**, one of the most potent inhibitors of ABCG2 found in literature to date. Reduction of the nitro function at R^3 resulting in an amine, decreased of the inhibitory activity significantly. Further reaction of the free amines with acid chlorides yielded substituted imines and amides. Unfortunately, this modification led to further reduction of the inhibitory activity.

Screening for ABCB1 and ABCC1 Inhibition. The selectivity toward ABCG2 was investigated by determining the inhibitory activity of some of the most potent compounds in the calcein AM assay using ABCB1 and ABCC1 overexpressing cell lines A2780adr and H69AR, respectively. Initial screening was carried out at a compound concentration of 10 μM measuring the increase of fluorescence resulting from intracellular calcein produced by the cleavage of the calcein AM esters over time. The standard inhibitor cyclosporine A (CsA) was used as positive control for both cell lines defining the state of "full inhibition". All tested compounds showed an inhibitory activity of less than 25% of the standard CsA and thus demonstrated a high selectivity toward ABCG2.

Determination of the Intrinsic Cytotoxicity via MTT Assay. Determination of the intrinsic cytotoxicity was carried out with parental and ABCG2 overexpressing MDCK II cells which were incubated with different dilutions of selected compounds. Cell viability was measured

after 72 h of incubation using 3-(4,5-dimethylthiazol-2-yl)-2,5-diphenyltetrazolium bromide (MTT) to detect the metabolic activity of the remaining viable cells. Reduction of MTT in living cells leads to the formation of a non water-soluble formazan species which can be detected colorimetrically. Further details are described in the experimental section. The half maximal growth inhibition (GI_{50}) is listed in Table 2 and representative concentration effect curves are shown in Figure 4. The therapeutic ratio ($TR = GI_{50}/IC_{50}$) was calculated from the GI_{50} value of a compound obtained with ABCG2 overexpressing cells.

For the unsubstituted basic structure **14**, containing a phenyl group at R^1, hydrogen at R^2 and nitro at R^3, a GI_{50} of 18.3 μM and a TR of 173 was found. For the analogue **52**, lacking the nitro group at R^3, a GI_{50} of 26.6 μM and a TR of 30.1 resulted. Despite of the increased toxicity caused by the 6-nitro substitution, the benefit of the high inhibitory potency of compound **14** becomes apparent yielding a TR that is more than three-fold higher than that of compound **59** (TR = 55.5). Compound **17** with phenyl group at R^1, 3'-methoxy at R^2 and nitro at R^3 displayed a pronounced cytotoxicity of 5.50 μM but still accomplished a TR of 166. Compound **18**, which is analogous to **17**, but contains 3',4'-dimethoxy at R^2, yielded a similar GI_{50} of 8.13 μM with a calculated TR of 220. In comparison, compound **53** without substitution with nitro at R^3 had a lower TR of 148. Another disubstituted derivative was investigated containing a phenyl group at R^1, 3'-nitro-4'-hydroxy at R^2 and nitro at R^3 (compound **23**). Due to its high inhibitory potency together with a GI_{50} of 13.2 μM a TR of 353 was found. Its analog **56**, without 6-nitro group, possessed a TR of 655, which was the highest ratio observed in our previous study.[27] Interestingly, the 2-pyridyl derivatives **28** and **29** showed almost no toxic effects with excellent GI_{50} values of 84.5 μM and 77.3 μM, respectively. This in accordance to our findings in the investigation of the cytotoxic effects of 4-anilino-2-pyridylquinazolines, where the pyridyl group was highly preferable over a phenyl group.[39] Moreover, for compound **29** the highest TR of 1212 among the investigated compounds was found.

Compounds **31**, **33** and **38** all contain a 3-trifluoromethylphenyl residue at R^1 and nitro at R^3. Unfortunately, low GI_{50} values around 3.5 μM resulted for **31** and **33** with 3'-hydroxy and 3',4'-dimethoxy substituents, respectively. The 3'-nitro-4'-hydroxy derivative possessed a considerably higher GI_{50} value of 27.4 μM resulting in a high TR of 830. In our previous study, the benefit of a 3-nitro-4-hydroxy substitution was already observed, illustrated by compound **52**. Also, the highly potent compounds **40** and **41**, both containing 3-methoxyphenyl at R^1 and 3'-nitro at R^3, were investigated. Compound **40** with 4'-cyano substituent at R^2 yielded a GI_{50} value of 11.0 μM resulting in a TR of 395, whereas the most potent compound **41** (3'-fluoro at R^2) unfortunately possessed a low GI_{50} value of 4.38 μM giving a TR of 187. Finally, compound **44** with a 3-pyridyl residue at R^1, 4'-methoxy at R^2 and amino at R^3 yielded a GI_{50} of 19.1 μM and giving the lowest TR of 29.6, which is due to a relatively high cytotoxicity along with a relatively low inhibitory potency.

Despite of the increased cytotoxicity caused by the nitro function in R^3, this modification shows its advantage in the context of inhibitory potency: the very low IC_{50} values found for the investigated 6-nitro derivatives led to high therapeutic ratios. The highest TR was found for compounds **28** and **29** containing a pyridyl group at position 2. It is notable, that a pyridyl substituent at position 2 led to only negligible intrinsic cytotoxicity but retained high inhibitory potency resulting in a remarkable TR.

Determination of the Ability to Reverse MDR via MTT Assay.

The ability to reverse the MDR toward the cytostatic drug SN-38 was investigated for compounds **23**, **28**, **29**, **38** and **41**. Different dilutions of the test compounds were added to the cells inhibiting the efflux of the cytostatic drug to a different extent. Inhibition of the transport protein therefore leads to a higher intracellular concentration of SN-38 and thus to a decreased cell viability. As positive control served MDCK II parental cells, representing the state of "full inhibition" due to the lack of ABCG2 expression.

Compounds **23** (IC_{50} = 37.4 nM), **28** (IC_{50} = 75.5 nM), **29** (IC_{50} = 63.8 nM), **38** (IC_{50} = 33.0 nM) and **41** (IC_{50} = 23.4 nM) were investigated in co-administration with the cytostatic drug SN-38. They were chosen due to their high inhibitory potency in the Hoechst 33342 accumulation assay (compounds **23, 38** and **41**) as well as their considerably low cytotoxic effects in the cell viability assay (compounds **28** and **29**). The shift of the pGI_{50} values toward the sensitive cells with increasing compound concentrations is depicted in Figure 5 a), c) and d) for selected compounds, indicated by the grey arrows. Full reversal of the MDR was achieved by all compounds at a concentration of about 1 µM obtaining approximately the same pGI_{50} value as the parental cells (Δ). To preclude unwanted transporter unspecific effects of the compound, an analogous assay was carried out using parental cells (Figure 5b). The resulting pGI_{50} values for each compound were all comparable giving no indication of unspecific effects. Based on the data derived from the graphs presented in Figure 5, the power of reversal of the compounds was calculated by plotting each pGI_{50} value of the corresponding concentration-viability curves against the logarithm of the compound concentration (Figure 6). Since the parental cells show no resistance against SN-38, they are expected to show the highest pEC_{50} values independently from the compound concentration with a low deviation among each concentration (○). In contrast, the BCRP overexpressing cells show a resistance dependent on the degree of inhibition by the compound. ABCG2 overexpressing cells without compound should obtain the lowest pEC_{50} value, increasing simultaneously with an increasing compound concentration (●). From the dose-effect plot it can be concluded, that all compounds reach a plateau at the same level as the sensitive cells. The EC_{50} values were calculated by nonlinear regression using the logistic equation to generate concentration-effect curves. By this method, for compound **23** an EC_{50} value of 34.0 nM, for **28** an EC_{50} value of 71.2 nM, for **29** an EC_{50} value of 48.3 nM for **38** an EC_{50} value of 57.0 nM and for **41** an EC_{50} value of 51.1 nM were calculated.

A second MDR reversal assay was carried out co-administering the cytostatic drug mitoxantrone (MX), which is also a substrate of ABCG2, with the two most potent compounds in the test set, namely **31** and **41**. The assay was carried out similar to the assay with SN-38, but using only MDCK II ABCG2 overexpressing cells. Different compound concentrations were investigated in the presence of 0.5 μM MX as well as in the absence of MX. The cell viability after an incubation period of 72 h is depicted in Figure 7 as bar chart. The control was performed using only cells without modulator in the absence and presence of MX. Increasing compound concentrations are expected to lead to an increasing sensitization of the cells toward MX, resulting in a decrease of the cell viability. At a concentration of 1 μM compounds **31** and **41** lead to full reversal of the MDR (Figure 7, light grey bars). Analogously EC_{50} values were derived for both compounds resulting in EC_{50} values of 21.8 nM and 19.5 nM for compound **31** and **41**, respectively. Cytotoxic effects of both compounds in the absence of MX can be observed by the decrease of the cell viability with increasing compound concentration (Figure 7, dark grey bars). However, cytotoxic effects are only noticeable at concentrations ≥ 1 μM. Both compounds show an excellent correlation between the EC_{50} resulting from the MDR reversal assay with MX and the Hoechst 33342 accumulation assay.

Investigation of ATPase activity. ATPase activity was measured using High Five insect cell membranes, which have previously been infected by baculovirus containing ABCG2 cDNA. The released inorganic phosphate, which is closely related to the transport activity of ABCG2 is detected by a colorimetric method. More details are provided in the experimental section.

Despite being an inhibitor of ABCG2, synthesized compounds could also be transported substrates of ABCG2 and therefore stimulate ATPase activity. In earlier studies of our working group we showed that closely related compounds displayed different behaviour in ATPase activity and enzyme kinetic investigations. To investigate the behaviour of the 6-nitro

derivatives we carried out vanadate-sensitive ATPase activity studies with highly potent compounds in Hoechst 33342 inhibition assay and compounds displaying structural similarities. The investigated compounds can be divided into three groups with different behaviour in ATPase activity assay, as illustrated in Table 3. Eight of the tested compounds had no observable effect on the ATPase activity in all tested concentrations (**14**, **17**, **21**, **31**, **32**, **37**, **41**, and **44**). This may be an indication that these compounds are not transported by ABCG2 and represent only inhibitors of ABCG2 detected in Hoechst 33342 accumulation assay. Another eight compounds showed a stimulation of ATPase activity, from which two compounds (**26** and **47**) possessed a strong activating effect to nearly the same extent as the standard activator quercetin. All other compounds were moderately stimulating ranging between 35 % and 52%. With regard to the potency of activation, five compounds had EC_{50} values, in the low nanomolar range (**18**, **20**, **28**, **30**, **40**), while one compound (**19**) showed an EC_{50} value in the range of quercetin and two compounds (**26**, **47)** possessed even higher values in the low micromolar range. Interestingly the two compounds with the highest activation contained both a *meta* methoxy substituent at the phenyl ring at position 4 of the quinazoline scaffold, but different substituents at positions 2 and 6.

Four compounds (**22**, **27**, **33**, **43**) showed a bell-shaped concentration-response curve with an activating effect at low concentrations and an inhibiting effect at higher concentrations. Inspection of the concentration of the maximal activity revealed one compound (**33**) in the low nanomolar range, one compound (**43**) with a concentration seven times higher and two compounds (**22**, **27**), with an about 30 times higher maximal concentration in the micromolar range. Inspection of the maximal stimulation (V_{max}) caused by the biphasic compounds showed that two compounds possessed a negligible effect of less than 30% (**27**, **43**). The other two compounds were ranging between 30% and 40% at the maximum. All biphasic compounds were not stimulating the ATPase activity very well. With the exception of compounds **26** and **47**, all investigated compounds showed low ATPase activity stimulation

or even no observable effect and can therefore be seen as very good inhibitors of ABCG2 with nearly no impact on ATPase activity. This is probably due to the nitro function at position 6 of the quinazoline scaffold as most quinazolines investigate so far stimulated ATPase activity. This modification leads to higher inhibitory potency in the Hoechst 33342 accumulation assay and no impact on ATPase activity.

Representative concentration-response curves of compounds **22** (biphasic), **26** (stimulating) and **quercetin** (activating standard) are illustrated in Figure 8. Compound **26** showed solely stimulation of ATPase activity over the whole range of concentrations similar to the standard activator quercetin. This activating effect on ATPase activity may point to substrate properties of the compound despite the inhibitory activity in the Hoechst 33342 accumulation assay. However, in earlier studies of our working group, the assumption of transport by ABCG2 in relation to ATPase activity stimulation, was challenged by a fluorescent heterodimeric ABCG2 inhibitor comprised of a quinazoline and chalcone moiety, which was also stimulating ATPase activity to a high extent. In confocal microscopy studies, this compound accumulated to the same extent in transfected MDCK II BCRP cells as in parenteral MDCK cells without the transporter protein, pointing to absence of transport.[40] For compound **22** a bell-shaped ATPase activity curve was observed. The occurrence of such bell-shaped curves is presumed to be due to two different binding sites for substrates. In most cases it is supposed that the activating and in some cases also transporting site has a high affinity for substrates and the inhibitory site has a low affinity for substrates.[41,42] The bell-shaped behaviour in ATPase activity can be due to the assumption that different binding pockets for one compound exist and the different behaviour of closely related structures with small differences in their substitution pattern lead to the proposal that multiple binding sites in ABCG2 protein must be present. This phenomenon can further be investigated by enzyme kinetic studies, which is illustrated in the following chapter.

Investigation of Interaction Type. Investigation of the interaction with the ABCG2 substrate Hoechst 33342 was carried out with compounds **17**, **31**, **40** and **41** that were selected according to their different ATPase profiles and their inhibitory potency in the Hoechst 33342 accumulation assay. For this purpose the ABCG2 overexpressing MDCK II cell line was used. Representative Lineweaver-Burk and Cornish-Bowden diagrams are depicted in Figure 9 together with a summary of the results from the Lineweaver-Burk diagrams in Table 4.

With exception of compound **31**, all other investigated compounds showed a non-competitive interaction with Hoechst 33342 according to the results of the Lineweaver-Burk method. Interestingly, all non-competitive interactions are of the "mixed-type", illustrated by the intersection of the lines in the second or third quadrant of the coordinate system. Although such "mixed-type" inhibitors bind differently from Hoechst 33342, they influence the active site, for instance by conformational changes of the protein. Compound **31** showed a competitive interaction with Hoechst 33342 for the same binding site, according to the intersection of the lines at the Y-axis of the plot. Representative Lineweaver-Burk plots for compounds **17**, **31**, **40** and **41** are illustrated in Figure 9 a, c, e and g. To confirm our results the direct linear plot according to Cornish-Bowden was carried out, since this method has been claimed to be less sensitive to outliers (Figure 9 b, d, f, h): a strong decrease of the maximum velocity V_{max} and roughly constant K_M values were found for compounds **17** and **41** with increasing concentrations, which is characteristic for a non-competitive interaction. In contrast, compound **31** displayed constant V_{max} values and increasing K_M values, which is characteristic for a competitive interaction. Simultaneously decreasing V_{max} and increasing K_M values confirmed the "mixed-type" properties of compound **40**. In our previous studies as well as in our ongoing work we discovered that a non-competitive interaction with Hoechst 33342 is the predominant mechanism for the quinazoline derivatives.[39] However, some substituents led to a rather competitive interaction with the substrate, which could be

explained by the different physicochemical properties of the compounds and for some by the ability to form hydrogen bonds *via* H-donor and H-acceptor-functions.

5D3 antibody binding assay. To get further insights into the interaction between the compounds and ABCG2 we performed a binding assay with conformation sensitive antibody 5D3 for selected derivatives. Therefor the monoclonal antibody PerCP-Cy^{TM}5.5 Mouse Anti-Human CD338 was used with the ABCG2 overexpressing PLB-985 cell line. The antibody is conjugated with a fluorescent dye and binds specifically to the CD338 epitope of ABCG2, dependent on the conformational state of the protein. We used the standard ABCG2 inhibitor **59** at a concentration of 10 µM as a reference due to its significant effect on antibody binding and set it as 100 % labelling of ABCG2. Furthermore, we used the ABCG2 substrate Hoechst 33342 for comparison, since it is known that substrates in most cases lead to a lower rate of antibody binding than inhibitors.[43] The unspecific binding of the antibody was taken into account by subtracting the fluorescence detected with an isotype-control.

We selected our most active compounds together with some 6-amino derivatives and conducted a screening at a compound concentration of 10 µM. The results are presented in Figure 10. The highest amount of labelling with the antibody was found for compound **17** (88%) which showed a non-competitive interaction with Hoechst 33342 in the interaction type studies. The lowest immunostaining with 5D3 antibody among the tested compounds was found for the 6-amino derivative **47** (47%), which is still higher than the labelling for the substrate Hoechst 33342 (35%). Although the differences in labelling among the remaining compounds were rather low, some tendencies were observable: compounds **43** and **44** which already exhibited different IC_{50} values, showed a different rate of labelling with the antibody of 72% and 84%, respectively. Compounds **31**, **33**, **40** and **41** gave a similar immunostaining of 66%, 58%, 62%, and 64%, respectively. There was no correlation between the IC_{50} value

of a compound and the rate of labelling with the antibody. However, the high rate of labelling with the antibody suggests that the compounds are no substrates of ABCG2.

Molecular docking

Docking of substrate Hoechst 33342. Very recently the cryo-EM structure of human ABCG2 has been reported and additionally in complex with a structural homolog of the standard inhibitor **59**.[44,45] Additionally a thorough discussion of the results of mutagenesis studies has been published.[46] Therefore we performed docking studies of selected compounds in order to gain insight into the molecular determinants involved in the formation of the receptor-substrate complex. First the substrate Hoechst 33342 was docked into the cryo-EM structure of the human ABCG2 and the interactions with the receptor were studied in detail. The results from docking studies show that putative binding modes of Hoechst 33342 occupy two binding sites S1 and S2 as depicted in Figure 11a. The site S1 is located at the interface between the two transmembrane domains and the site S2 is between the transmembrane regions. As shown in Figure 11b, 64% of docked poses of Hoechst 33242 occupied site S1 and the remaining 36% of poses were occupying site S2. The previously published literature specified that the site S1 is highly promiscuous allowing substrates and non-substrates to dock in a wide variety of binding poses.[47] On contrary, the site S2 is highly selective and favoring substrates in comparison to non-substrates or inhibitors. The new cryo-EM structure (Jackson et. al) specified that the site S1 is occupied by the fumitremorgin C-related inhibitor, MZ29.[45] According to interaction type analysis we had found a non-competitive mixed-type interaction of compound **59** and Hoechst 33342. Thus, we considered the binding poses of Hoechst 33342 docked at the site S2 for our analysis.

The 2D interaction diagram of the putative binding pose of Hoechst 33342 is shown in Figure 11c. Hoechst 33342 has many functional groups that could potentially interact with the receptor. The nitrogen in the methylpiperazine might acts as a donor and possibly interacts

with the main chain of the residue Gly179. The benzimidazole group attached to the methylpiperazine is positioned at the edge of the transmembrane domain and either N1 or N3 of the benzimidazole group act as donor and acceptor and interact with Asn387. The amino acid Ans387 is from connecting helix the interface between the transmembrane and nucleotide binding domains and plays an important role for the efflux function of the receptor. The finding was confirmed by the negative effects of N397A mutant on receptor efflux activity with Hoechst 33342 as substrate.[48] The mutagenesis study also suggests that the positioning of Asn387 at the interface could be vital for communication between the two domains. The second benzimidazole group is surrounded by hydrophobic residues Leu338, Leu447, Val450 and polar residues Asn387, Asn391, Glu451 and Asp477. The ethoxyphenyl group is located in a subpocket formed by Gln398, Ser443, Glu446, Met481, and Arg482. Among the residues, the side chains of Gln398, Ser443 and Arg482 interact with the ethoxyphenyl group of Hoechst 33342. The results from different mutagenesis studies specified that the overall efflux activity was decreased for the mutants Q398A, R482G and R482T.[48,49,50,51] The mutants also show a decreasing effect on the ATPase activity. An aromatic residue Tyr489 located at a distance of approximately 6 Å might act as an edge for the binding site and position the substrate Hoechst 33342 inside the binding pocket. The mutagenesis studies by Tamura et al. show decrease in efflux and ATPase activity for the F489L mutant.[52] This indicates that an aromatic residue is required for strong hydrophobic interaction between Hoechst 33342 and the amino acids inside the substrate binding pocket .

Docking of inhibitors. To explore binding modes for the quinazoline derivatives and identify a possible explanation for the mechanism of inhibition, we selected compounds **31** and **41** for performing molecular docking studies in the cryo-EM structure of the ABCG2 receptor. Compound **31** was selected as it showed competitive type of interaction with Hoechst 33342

while Compound **41** was the most potent compound showing non-competitive type of interaction (table 4).

Similar to Hoechst 33342, compound **31** can be accommodated in the binding site S1 and S2 (Figure 12a). In our docking results, only 6% of poses of compound **31** occupied the site S1 and the remaining 94% of poses were occupied site S2. In particular, the best scoring binding poses were bound near the connecting helix between the transmembrane and nucleotide binding domain. The 2D interaction diagram of putative binding pose with the receptor is shown in Figure 12b. The quinazoline moiety of **31** is placed below the ionic lock formed between Asp127 and Lys453. The 3-CF_3-phenyl group is located in the subpocket formed by the residues Val449, Val450, Lys452, Lys453 and Ser532. The NH of the 3-hydroxyaniline group possibly forms interaction with the main chain of Asp128. In particular, the hydroxyl substituent at position 3 of the aniline group acts as hydrogen bond donor and acceptor which forms strong interaction with the main chain of Val450 and Leu454. Additionally, the nitro group at position 6 of the quinazoline moiety forms electrostatic interactions with the side chain of Arg191 and the main chain of Asp128. The obtained docked poses suggest that compound **31** possibly binds at the site S1 which is closer to the substrate banding site and exhibits competitive type of inhibition.

As a next step, we analyzed the binding poses of compound **41** which displayed non-competitive and mixed type of inhibition. The putative binding poses and the interaction with the receptor are shown in Figure 12c and d. The results from docking show that all 100 binding poses were docked to the site S2. Similar to the bound inhibitor, MZ29 in the cryo-EM structure it occupied the binding site S2 interface between the two transmembrane domains. The quinazoline moiety forms a strong aromatic π-π interaction with Phe439. The nitro group substituted at position 6 of the quinazoline moiety forms electrostatic interactions with Asn436. The NH-group of the 3-fluoro-aniline group forms hydrogen bond interaction with Met549. The phenyl ring is positioned in a subpocket formed by the hydrophobic

residues Phe431, Phe432, Thr435, Met549 and Leu555. The 3-methoxyphenyl group forms a π-stacking with another aromatic residue Phe439. Based on the analysis of binding poses and interaction from docking studies, compound **41** occupies the site S2 and shows non-competitive or mixed-type of interaction with the substrate Hoechst 33242.

Conclusions

This study is a continuation of our previous investigations of 2,4-disubstituted-quinazolines. Extraordinary low IC_{50} values resulted from introducing a nitro group at position 6 of a 2,4-disubstituted quinazoline scaffold. Further substitution with methoxy residues at the aromatic rings at position 2 and 4 of the scaffold increased the potency toward ABCG2 even more. The highest potency in the Hoechst 33342 accumulation assay resulted for compound **41** from a substitution with 3-methoxyphenyl at position 2 and 3'-fluoroaniline at position 4. It was determined to be about 10-fold more potent than compound **59**, one of the most potent inhibitors of ABCG2 found in literature. Reduction of the nitro function at position 6 yielded derivatives with an amino group with significantly lower potencies than the corresponding 6-nitro derivatives. Reaction of the amino function at position 6 with acid chlorides yielded aromatic amides with unfortunately even further decreased inhibitory potency. We concluded that the nitro function is preferable over amino groups and amido groups.

Moreover, the screening of selected compounds in a calcein AM assay against the transport proteins ABCB1 and ABCC1 showed their high selectivity toward ABCG2. Resulting activities toward both transport proteins were below 25% of the response observed by the control cyclosporine A confirming the specificity of the inhibitors. Investigation of the intrinsic cytotoxicity showed slightly increased toxic effects for the 6-nitro derivatives compared to their analogs lacking the nitro group. Generally aromatic nitro groups are considered as toxicologically problematic. Most nitro-containing compounds can cause

methaemoglobinemia and are potentially mutagenic.[53] However, a prominent exception from this rule are calcium channel blockers of the dihydropyridine type. Therefore additional toxicological studies are necessary to explore the feasibility of future *in vivo* studies of the ABCG2 inhibitors. The calculated therapeutic ratios (GI_{50}/IC_{50}) still were relatively high due to the high inhibitory potencies of the compounds. Most notably a substitution with pyridyl at position 2 turned out to be highly beneficial (see compounds **28** and **29**), leading to a therapeutic ratio which is up to 22-fold higher than that of compound **59**. Moreover, most potent compounds were investigated for their ability to reverse MDR toward the cytostatic drugs SN-38 and mitoxantrone using ABCG2 overexpressing MDCK II BCRP cells. All tested compounds were able to reverse the MDR restoring the sensitivity toward SN-38 and mitoxantrone at low compound concentrations. Full reversal of the MDR was achieved by all compounds at compound concentrations of about 1 μM. Investigation of the ATPase activity of selected compounds resulted in three different groups: more than one third of the compounds showed no effect on ATPase activity. This may be an indication that these compounds are not transported by ABCG2 and represent only inhibitors of ABCG2 as detected in Hoechst 33342 accumulation assay. Four compounds showed biphasic ATPase activity curves with an activating/stimulating site at low concentrations and an inhibitory site at higher concentrations (see compounds **22**, **27**, **33** and **43**). It is reasonable that different binding regions with different affinities are present in ABCG2. The third group consists of eight compounds with stimulation of ATPase activity, of which almost all showed low stimulation with exception of compounds **26** and **47**. These two compounds both contain a *meta* methoxy group at the phenyl ring at position 4 of the quinazoline scaffold and showed the same stimulating effect as the standard stimulator quercetin. The nitro substitution at position 6 of the quinazoline scaffold seems to lead to higher inhibitory potencies in the Hoechst 33342 accumulation assay and leads to low or no impact on ATPase activity.

Furthermore, the type of interaction with Hoechst 33342 was determined for selected compounds using the methods according to Lineweaver-Burk and Cornish-Bowden. Interestingly, the investigated compounds showed different types of interaction with Hoechst 33342 but were mostly non-competitive, meaning that they bind apart from Hoechst 33342. Some compounds showed competitive portions, which is characteristic for "mixed-type" inhibitors or pure competitive inhibitors. Here, one compound (compound **31**) was found to compete for the same binding site as Hoechst 33342.

Additionally the conformation sensitive 5D3 antibody binding assay was carried out to monitor the conformational change of ABCG2 in the presence of selected compounds. All compounds induced a higher level of immunostaining with the antibody than the ABCG2 substrate Hoechst 33342. Only small differences in the rate of labelling resulted for the investigated compounds, whereas no correlation was found with the IC_{50} values from the Hoechst 33342 accumulation assay.

As a logical continuation of our earlier work, the quinazoline scaffold was further modified and functionalized giving more insights into the SAR of this compound class. The study yielded several compounds with extraordinary high inhibitory potencies and selectivity toward ABCG2. Based on the promising *in vitro* results, particularly their ability to reverse MDR toward SN-38 and MX, further *in vivo* studies should be interesting. Furthermore, molecular modelling studies based on recently published cryo-EM structures of ABCG2 supported the results of the substrate and inhibitors obtained by biological and kinetic studies.

Experimental Section

Chemistry. Materials. Chemicals were purchased from Acros Organics (Geel, Belgium), Alfa Aesar (Karlsruhe, Germany), Sigma Aldrich (Steinheim, Germany) or Merck (Darmstadt, Germany) and used without further purification. Microwave reactions were carried out in 50 mL vials using a CEM Discover SP (CEM GmbH, Kamp-Lintfort, Germany) and monitored

by thin layer chromatography (TLC) employing an aluminium plate coated with silica gel 60 F_{254} (Merck Millipore, Billerica, MA, USA). For the preparation of the TLC a mixture of dichloromethane and methanol in the ratio of 9:1 was used as eluent. Following, the plates were analyzed in a UV cabinet at an excitation wavelength of 254 nm. Identity of the test compounds was confirmed by NMR with the ^{1}H- and ^{13}C spectra obtained on a Bruker Advance 500 MHz (500/126 MHz) or Bruker Advance 600 MHz (600/151 MHz), respectively. Chemical shifts (δ) relating to the internal standard DMSO-d6, also used as solvent for the compounds, are expressed in ppm. For the assignment of the ^{13}C signals distortionless enhancement by polarization transfer (DEPT) as well as attached proton test (APT) was applied. Multiplicity of the signals are given as singlet (s), doublet (d), doublet of doublets (dd), triplet of doublets (td), triplet (t), doublet of triplets (dt), quartet (q) and multiplet (m) whereas the coupling constants J are given in Hz. The purity of all biologically evaluated compounds was determined to be >95% by elemental analysis recorded on a Vario EL V24 CHN Elemental Analyzer (Elementar Analysensysteme GmbH, Hanau, Germany). Found values were in the range of ±0.4% of the theoretical values, unless indicated

2-amino-5-nitrobenzamide (1).

To a solution of 2-amino-5-nitrobenzoic acid (1.80 g, 10 mmol) in 100 mL dry tetrahydrofuran was slowly added triphosgene (1.19 g, 4 mmol) while stirring at room temperature. The mixture was then refluxed under moisture exclusion for 3 h. Under stirring, a constant stream of ammonia gas was bubbled through the mixture for 30 min at 50 °C. Then, 50 mL of water was added and the precipitate filtered off. Additional product was obtained by concentrating the mixture under reduced pressure to one half of the initial volume to yield **1** as bright yellow crystals (1.58 g, 87%). ^{1}H NMR (500 MHz, DMSO-d_6) δ 12.97 (s, 1H), 8.84 (d, J = 2.7 Hz, 1H), 8.56 (dd, J = 9.0, 2.7 Hz, 1H), 8.27 – 8.19 (m, 2H), 7.92 (d, J = 9.0 Hz, 1H), 7.68 – 7.62 (m, 1H), 7.58 (dd, J = 8.3, 6.7 Hz, 2H). ^{13}C NMR (126 MHz, DMSO) δ

160.74, 155.16, 152.43, 144.86, 132.40, 128.86, 128.65, 128.24, 127.99, 126.66, 122.18, 121.22.

General Procedure for the Preparation of compounds 2-7. A mixture of 2-amino-5-nitrobenzamide **1** (3.62 g, 20 mmol), the corresponding aldehyde derivative (20 mmol), iodine (3.17 g, 25 mmol), anhydrous potassium carbonate (2.76 g, 20 mmol) and 20 ml DMF was stirred at 90-110 °C for 8-24 h. The end of the reaction was monitored by TLC and the mixture poured on crushed ice to form a precipitate. Incomplete precipitation can be prevented by adjusting the pH with concentrated HCl solution to 7. After filtration of the precipitate, it was thoroughly washed with 100 mL of a 20% sodium thiosulfate solution followed by 100 mL of hot distilled water. Purification was performed by recrystallization from ethanol.

6-nitro-2-phenylquinazolin-4(3H)-one (2). The compound was synthesized from **1** (3.62 g, 20 mmol) and benzaldehyde (2.12 g, 20 mmol) as described in the general procedure for compounds **2-7** to yield **2** as a yellow solid (3.85 g, 72%). ^{1}H NMR (500 MHz, DMSO-d_6) δ 12.97 (s, 1H), 8.84 (d, J = 2.7 Hz, 1H), 8.56 (dd, J = 9.0, 2.7 Hz, 1H), 8.27 – 8.19 (m, 2H), 7.92 (d, J = 9.0 Hz, 1H), 7.68 – 7.62 (m, 1H), 7.58 (dd, J = 8.3, 6.7 Hz, 2H). ^{13}C NMR (126 MHz, DMSO) δ 144.86, 132.40, 132.24, 128.86, 128.65, 128.39, 122.18.

6-nitro-2-(pyridin-3-yl)quinazolin-4(3H)-one (3). The compound was synthesized from **1** (3.62 g, 20 mmol) and nicotinaldehyde (2.14 g, 20 mmol) as described in the general procedure for compounds **2-7** to yield **3** as a yellow-orange solid (3.70 g, 69%). ^{1}H NMR (500 MHz, DMSO-d_6) δ 9.58 – 9.44 (m, 1H), 8.82 (d, J = 2.8 Hz, 1H), 8.67 (dt, J = 7.9, 2.0 Hz, 1H), 8.61 (dd, J = 4.9, 1.7 Hz, 1H), 8.24 (dd, J = 9.0, 2.8 Hz, 1H), 7.94 (s, 1H), 7.58 (d, J = 9.0 Hz, 1H), 7.45 (ddd, J = 7.9, 4.7, 0.8 Hz, 1H). ^{13}C NMR (126 MHz, DMSO) δ 171.52,

163.89, 162.42, 156.83, 150.48, 149.70, 141.89, 135.45, 135.21, 127.35, 125.06, 123.24, 120.82.

6-nitro-2-(pyridin-4-yl)quinazolin-4(3H)-one (4). The compound was synthesized from **1** (3.62 g, 20 mmol) and isonicotinaldehyde (2.14 g, 20 mmol) as described in the general procedure for compounds **2-7** to yield **4** as a yellow solid (2.74 g, 51%). ^{1}H NMR (500 MHz, DMSO-d_6) δ 13.18 (s, 1H), 8.82 (dd, J = 8.1, 4.1 Hz, 3H), 8.57 (dd, J = 9.2, 2.7 Hz, 1H), 8.16 – 8.07 (m, 2H), 7.95 (d, J = 9.3 Hz, 1H). ^{13}C NMR (126 MHz, DMSO) δ 161.62, 154.18, 152.54, 150.51, 145.35, 139.58, 129.56, 128.73, 122.09, 121.96, 121.77.

6-nitro-2-(3-(trifluoromethyl)phenyl)quinazolin-4(3H)-one (5). The compound was synthesized from **1** (3.62 g, 20 mmol) and 3-(trifluoromethyl)benzaldehyde (3.48 g, 20 mmol) as described in the general procedure for compounds **2-7** to yield **5** as a yellow solid (5.16 g, 77%). ^{1}H NMR (500 MHz, DMSO-d_6) δ 13.18 (s, 1H), 8.82 (d, J = 2.7 Hz, 1H), 8.59 – 8.53 (m, 2H), 8.50 (ddd, J = 8.2, 2.0, 1.1 Hz, 1H), 8.00 (ddt, J = 7.9, 1.9, 1.0 Hz, 1H), 7.97 – 7.91 (m, 1H), 7.87 – 7.77 (m, 1H). ^{13}C NMR (126 MHz, DMSO) δ 161.67, 154.51, 152.69, 145.07, 133.26, 132.33, 130.07, 129.61 (d, J = 32.3 Hz), 129.37, 128.71 (d, J = 3.5 Hz), 128.65, 127.25, 125.04 (d, J = 3.8 Hz), 122.92, 122.07, 121.36.

2-(3-methoxyphenyl)-6-nitroquinazolin-4(3H)-one (6). The compound was synthesized from **1** (3.62 g, 20 mmol) and 3-methoxybenzaldehyde (2.72 g, 20 mmol) as described in the general procedure for compounds **2-7** to yield **6** as a yellow solid (4.88 g, 82%). ^{1}H NMR (500 MHz, DMSO-d_6) δ 12.94 (s, 1H), 8.83 (d, J = 2.7 Hz, 1H), 8.52 (dd, J = 9.0, 2.8 Hz, 1H), 7.88 (d, J = 8.9 Hz, 1H), 7.85 (ddd, J = 7.8, 1.7, 0.9 Hz, 1H), 7.80 (t, J = 2.2 Hz, 1H), 7.47 (t, J = 8.0 Hz, 1H), 7.18 (ddd, J = 8.2, 2.6, 0.9 Hz, 1H), 3.86 (s, 3H). ^{13}C NMR (126 MHz,

DMSO) δ 161.65, 161.42, 159.51, 153.03, 144.84, 142.84, 133.43, 130.00, 128.61, 122.13, 120.75, 118.60, 113.11, 55.59.

2-(3,4-dimethoxyphenyl)-6-nitroquinazolin-4(3H)-one (7). The compound was synthesized from **1** (3.62 g, 20 mmol) and 3,4-dimethoxybenzaldehyde (3.32 g, 20 mmol) as described in the general procedure for compounds **2-7** to yield **7** as a yellow solid (4.19 g, 64%). ^{1}H NMR (500 MHz, DMSO-d_6) δ 12.81 (s, 1H), 8.80 (d, J = 2.7 Hz, 1H), 8.50 (dd, J = 9.0, 2.8 Hz, 1H), 7.94 (dd, J = 8.5, 2.2 Hz, 1H), 7.88 – 7.82 (m, 2H), 7.13 (d, J = 8.7 Hz, 1H), 3.88 (s, 3H), 3.85 (s, 3H). ^{13}C NMR (126 MHz, DMSO) δ 162.24, 155.65, 153.41, 152.49, 148.72, 144.28, 128.86, 128.42, 124.35, 122.24, 122.18, 120.68, 111.58, 111.20, 55.89, 55.87.

General Procedure for the Preparation of compounds 8-13. The corresponding 2-substituted 6-nitroquinazolin-4(3*H*)-one derivative **2-7** (10 mmol) was added to phosphorous oxychloride (30 mL, 0.32 mol) and stirred for 10 min at room temperature. The mixture was then refluxed for 4-12 h and the reaction monitored by TLC. After completion of the reaction, excess $POCl_3$ was removed under reduced pressure and 50 mL ice water added. Subsequently, 50 mL DCM was added while stirring and the pH of the mixture slowly adjusted to 7 with 25% ammonium solution. With a separatory funnel, the organic phase was collected, washed with 50 mL brine and dried over $MgSO_4$. The solvent was removed under reduced pressure and the obtained solid recrystallized from isopropanol.

3-(6-nitro-4-oxo-3,4-dihydroquinazolin-2-yl)benzonitrile (8). The compound was synthesized from **2** (2.67 g, 10 mmol) as described in the general procedure for compounds **8-13** to yield **8** as a yellow solid (2.46 g, 86%). ^{1}H NMR (500 MHz, DMSO-d_6) δ 8.83 (d, J = 2.7 Hz, 1H), 8.55 (dd, J = 9.0, 2.8 Hz, 1H), 8.24 – 8.19 (m, 2H), 7.91 (d, J = 9.0 Hz, 1H), 7.67

– 7.62 (m, 1H), 7.60 – 7.55 (m, 2H). ^{13}C NMR (126 MHz, DMSO) δ 161.74, 155.85, 152.97, 144.85, 132.41, 132.16, 129.19, 128.85, 128.64, 128.39, 122.16, 121.14.

4-chloro-6-nitro-2-(pyridin-3-yl)quinazoline (9). The compound was synthesized from **3** (2.68 g, 10 mmol) as described in the general procedure for compounds **8-13** to yield **9** as an orange solid (2.38 g, 83%). ^{1}H NMR (500 MHz, DMSO-d_6) δ 9.38 (dd, J = 2.3, 0.8 Hz, 1H), 8.88 (dd, J = 5.0, 1.6 Hz, 1H), 8.82 (d, J = 2.7 Hz, 1H), 8.72 (ddd, J = 8.1, 2.3, 1.6 Hz, 1H), 8.60 – 8.54 (m, 1H), 7.94 (d, J = 8.8 Hz, 1H), 7.79 (ddd, J = 8.1, 5.1, 0.8 Hz, 1H). ^{13}C NMR (126 MHz, DMSO) δ 161.49, 153.56, 152.52, 150.29, 147.22, 145.21, 138.43, 129.36, 129.20, 128.77, 124.70, 122.09, 121.42.

4-chloro-6-nitro-2-(pyridin-4-yl)quinazoline (10). The compound was synthesized from **4** (2.68 g, 10 mmol) as described in the general procedure for compounds **8-13** to yield **10** as an orange solid (2.12 g, 74%). ^{1}H NMR (500 MHz, DMSO-d_6) δ 13.21 (s, 1H), 8.85 – 8.81 (m, 2H), 8.57 (dd, J = 9.0, 2.7 Hz, 1H), 8.18 – 8.10 (m, 2H), 7.95 (d, J = 9.0 Hz, 1H). ^{13}C NMR (126 MHz, DMSO) δ 161.55, 153.98, 152.46, 150.07, 145.44, 140.03, 129.63, 128.80, 122.10, 121.81.

4-chloro-6-nitro-2-(3-(trifluoromethyl)phenyl)quinazoline (11). The compound was synthesized from **5** (3.35 g, 10 mmol) as described in the general procedure for compounds **8-13** to yield **11** as a yellow solid (3.18 g, 90%). ^{1}H NMR (600 MHz, DMSO-d_6) δ 8.81 (d, J = 2.7 Hz, 1H), 8.59 – 8.52 (m, 2H), 8.52 – 8.46 (m, 1H), 8.03 – 7.97 (m, 1H), 7.94 (d, J = 8.9 Hz, 1H), 7.82 (t, J = 7.9 Hz, 1H). ^{13}C NMR (151 MHz, DMSO) δ 161.68, 154.53, 152.67, 145.14, 133.24, 132.40, 130.14, 129.66 (d, J = 32.5 Hz), 129.42, 128.80 (d, J = 3.8 Hz), 128.74, 125.09 (t, J = 3.9 Hz), 123.16, 122.13, 121.40.

4-chloro-2-(3-methoxyphenyl)-6-nitroquinazoline (12). The compound was synthesized from **6** (2.97 g, 10 mmol) as described in the general procedure for compounds **8-13** to yield **12** as a yellow solid (2.81 g, 89%). ^{1}H NMR (500 MHz, DMSO-d_6) δ 8.83 (d, J = 2.7 Hz, 1H), 8.55 (dd, J = 9.0, 2.8 Hz, 1H), 7.92 (d, J = 9.0 Hz, 1H), 7.83 (ddd, J = 7.7, 1.7, 0.9 Hz, 1H), 7.78 (dd, J = 2.6, 1.7 Hz, 1H), 7.49 (t, J = 8.0 Hz, 1H), 7.20 (ddd, J = 8.2, 2.6, 0.9 Hz, 1H), 3.87 (s, 3H). ^{13}C NMR (126 MHz, DMSO) δ 161.74, 159.51, 155.56, 152.89, 144.87, 133.42, 130.02, 129.23, 128.65, 122.15, 121.18, 120.77, 118.63, 113.14, 55.61.

4-chloro-2-(3,4-dimethoxyphenyl)-6-nitroquinazoline (13). The compound was synthesized from **7** (3.27 g, 10 mmol) as described in the general procedure for compounds **8-13** to yield **13** as a yellow solid (2.75 g, 71%). ^{1}H NMR (500 MHz, DMSO-d_6) δ 8.79 (d, J = 2.7 Hz, 1H), 8.50 (dd, J = 9.0, 2.7 Hz, 1H), 7.92 (dd, J = 8.5, 2.2 Hz, 1H), 7.89 – 7.77 (m, 2H), 7.13 (d, J = 8.6 Hz, 1H), 3.88 (s, 3H), 3.85 (s, 3H). ^{13}C NMR (126 MHz, DMSO) δ 161.80, 155.29, 153.05, 152.61, 148.73, 144.43, 128.80, 128.59, 123.85, 122.26, 122.19, 120.66, 111.60, 111.20, 55.91, 55.89.

General Procedure for the Preparation of compounds 14-42. The corresponding 2 substituted 4-chloroquinazoline **8-13** (1 mmol) and a substituted aniline (1 mmol) were added to a 50 mL microwave tube and suspended in 25 mL isopropanol. The tube was sealed and the reaction mixture stirred under 100 watt microwave irradiation at 110 °C for 20-40 min. Completion of the reaction was monitored by TLC. After cooling, a precipitate was formed and filtered off by suction. Recrystallization was carried out from ethanol.

6-nitro-N,2-diphenylquinazolin-4-amine (14). The compound was synthesized according to the general procedure for compounds **14-42** from **8** (2.86 g, 10 mmol) and aniline (0.93 g, 10 mmol) to yield **14** as an orange solid (2.40 g, 70%), mp 264-265 °C. ^{1}H NMR (500 MHz,

DMSO-d_6) δ 10.47 (s, 1H), 9.65 (d, J = 2.5 Hz, 1H), 8.53 (dd, J = 9.2, 2.5 Hz, 1H), 8.46 – 8.36 (m, 2H), 7.96 (d, J = 9.2 Hz, 1H), 7.94 – 7.89 (m, 2H), 7.58 – 7.44 (m, 5H), 7.23 (tt, J = 7.4, 1.1 Hz, 1H). ^{13}C NMR (126 MHz, DMSO) δ 162.32, 159.06, 154.21, 144.24, 138.67, 137.59, 131.33, 129.68, 128.69, 128.49, 126.90, 124.59, 122.90, 121.05, 113.35. Anal. Calcd. for $C_{20}H_{14}N_4O_2$: C, 70.17; H, 4.12; N, 16.37. Found: C, 70.32; H, 4.26; N, 16.17.

3-((6-nitro-2-phenylquinazolin-4-yl)amino)phenol (15). The compound was synthesized according to the general procedure for compounds **14-42** from **8** (2.86 g, 10 mmol) and 3-aminophenol (1.09 g, 10 mmol) to yield **15** as a yellow solid (2.39 g, 66%), mp 277-278 °C (decomp.). ^{1}H NMR (500 MHz, DMSO-d_6) δ 10.35 (s, 1H), 9.67 (d, J = 2.4 Hz, 1H), 9.53 (s, 1H), 8.53 (dd, J = 9.2, 2.5 Hz, 1H), 8.49 – 8.41 (m, 2H), 7.96 (d, J = 9.1 Hz, 1H), 7.57 – 7.48 (m, 3H), 7.43 (t, J = 2.2 Hz, 1H), 7.38 (ddd, J = 8.1, 2.1, 1.0 Hz, 1H), 7.26 (t, J = 8.0 Hz, 1H), 6.64 (ddd, J = 8.1, 2.4, 1.0 Hz, 1H). ^{13}C NMR (126 MHz, DMSO) δ 162.38, 159.03, 157.67, 154.22, 144.25, 139.70, 137.63, 131.33, 129.67, 129.29, 128.67, 128.60, 126.89, 121.11, 113.59, 113.41, 111.76, 109.95. Anal. Calcd. for $C_{20}H_{14}N_4O_3$: C, 67.03; H, 3.94; N, 15.63. Found: C, 67.24; H, 4.17; N, 15.41.

4-((6-nitro-2-phenylquinazolin-4-yl)amino)benzene-1,2-diol (16). The compound was synthesized from a solution of **18** (4.02 g, 10 mmol) in dry DCM kept at – 60 °C under moisture exclusion. Boron tribromide was slowly added under stirring via a dropping funnel within 30 min and the cooling bath removed. After another 12 h stirring at room temperature, the solvent was evaporated under reduced pressure and the obtained solid recrystallized from 75 % ethanol to yield **16** as red solid (3.14 g, 84%), mp >300 °C. ^{1}H NMR (500 MHz, DMSO-d_6) δ 10.27 (s, 1H), 9.62 (d, J = 2.5 Hz, 1H), 9.07 (s, 1H), 8.86 (s, 1H), 8.52 (dd, J = 9.2, 2.5 Hz, 1H), 8.47 – 8.39 (m, 2H), 7.93 (d, J = 9.2 Hz, 1H), 7.56 – 7.48 (m, 3H), 7.34 (d, J = 2.5 Hz, 1H), 7.14 (dd, J = 8.5, 2.5 Hz, 1H), 6.82 (d, J = 8.5 Hz, 1H). ^{13}C NMR (126 MHz,

DMSO) δ 162.48, 158.90, 154.19, 145.08, 144.09, 142.75, 137.70, 131.25, 130.22, 129.42, 128.61, 128.59, 126.77, 121.02, 115.24, 114.44, 113.35, 111.57. Anal. Calcd. for $C_{20}H_{14}N_4O_4$: C, 64.17; H, 3.77; N, 14.97. Found: C, 64.15; H, 3.67; N, 14.67.

N-(3-methoxyphenyl)-6-nitro-2-phenylquinazolin-4-amine (17). The compound was synthesized according to the general procedure for compounds **14-42** from **8** (2.86 g, 10 mmol) and 3-methoxyaniline (1.23 g, 10 mmol) to yield **17** as an orange solid (2.20 g, 59%), mp 242-243 °C. ^{1}H NMR (600 MHz, DMSO-d_6) δ 10.42 (s, 1H), 9.66 (d, J = 2.4 Hz, 1H), 8.53 (dd, J = 9.1, 2.4 Hz, 1H), 8.49 – 8.39 (m, 2H), 7.97 (d, J = 9.1 Hz, 1H), 7.67 (s, 1H), 7.62 – 7.48 (m, 4H), 7.38 (t, J = 8.1 Hz, 1H), 6.80 (dd, J = 8.1, 2.4 Hz, 1H), 3.83 (s, 3H). ^{13}C NMR (151 MHz, DMSO) δ 162.27, 159.53, 158.98, 154.18, 144.28, 139.95, 137.61, 131.39, 129.73, 129.41, 128.67, 128.47, 126.93, 121.02, 114.87, 113.40, 110.49, 108.09, 55.30. Anal. Calcd. for $C_{21}H_{16}N_4O_3$: C, 67.73; H, 4.33; N, 15.05. Found: C, 67.48; H, 4.25; N, 14.85.

N-(3,4-dimethoxyphenyl)-6-nitro-2-phenylquinazolin-4-amine (18). The compound was synthesized according to the general procedure for compounds **14-42** from **8** (2.86 g, 10 mmol) and 3,4-dimethoxyaniline (1.53 g, 10 mmol) to yield **18** as a red-orange solid (3.10 g, 77%), mp 238-240 °C. ^{1}H NMR (500 MHz, DMSO-d_6) δ 10.35 (s, 1H), 9.63 (d, J = 2.5 Hz, 1H), 8.51 (dd, J = 9.2, 2.4 Hz, 1H), 8.49 – 8.42 (m, 2H), 7.94 (d, J = 9.2 Hz, 1H), 7.68 (d, J = 2.5 Hz, 1H), 7.57 – 7.47 (m, 3H), 7.43 (dd, J = 8.7, 2.4 Hz, 1H), 7.06 (d, J = 8.7 Hz, 1H), 3.83 (s, 3H), 3.81 (s, 3H). ^{13}C NMR (126 MHz, DMSO) δ 162.36, 158.78, 154.19, 148.45, 145.98, 144.16, 137.71, 131.99, 131.31, 129.60, 128.60, 128.46, 126.81, 120.91, 114.76, 113.35, 111.85, 107.81, 55.89, 55.66. Anal. Calcd. for $C_{22}H_{18}N_4O_4$: C, 65.66; H, 4.51; N, 13.92. Found: C, 65.74; H, 4.88; N, 13.55.

3-((6-nitro-2-phenylquinazolin-4-yl)amino)benzonitrile (19). The compound was synthesized according to the general procedure for compounds **14-42** from **8** (2.86 g, 10 mmol) and 3-aminobenzonitrile (1.18 g, 10 mmol) to yield **19** as a yellow solid (2.98 g, 81%), mp >300 °C. ^{1}H NMR (500 MHz, DMSO-d_6) δ 11.03 (s, 1H), 9.69 (d, J = 2.4 Hz, 1H), 8.59 (dd, J = 9.2, 2.4 Hz, 1H), 8.48 – 8.31 (m, 3H), 8.24 (dt, J = 7.5, 2.1 Hz, 1H), 8.11 (d, J = 9.1 Hz, 1H), 7.78 – 7.65 (m, 2H), 7.64 – 7.47 (m, 3H). ^{13}C NMR (126 MHz, DMSO) δ 161.54, 159.13, 152.28, 144.68, 139.27, 136.16, 132.05, 130.19, 128.83, 128.70, 128.48, 128.22, 127.67, 127.57, 126.17, 121.14, 118.71, 113.20, 111.57. Anal. Calcd. for $C_{21}H_{13}N_5O_2$: C, 68.66; H, 3.57; N, 19.06. Found: C, 68.70; H, 3.90; N, 18.75.

4-((6-nitro-2-phenylquinazolin-4-yl)amino)benzonitrile (20). The compound was synthesized according to the general procedure for compounds **14-42** from **8** (2.86 g, 10 mmol) and 4-aminobenzonitrile (1.18 g, 10 mmol) to yield **20** as a yellow solid (2.53 g, 69%), mp >300 °C. ^{1}H NMR (600 MHz, DMSO-d_6) δ 10.93 (s, 1H), 9.71 (d, J = 2.4 Hz, 1H), 8.60 (dd, J = 9.2, 2.4 Hz, 1H), 8.47 – 8.41 (m, 2H), 8.22 – 8.14 (m, 2H), 8.08 (d, J = 9.1 Hz, 1H), 7.99 – 7.92 (m, 2H), 7.61 – 7.52 (m, 3H). ^{13}C NMR (151 MHz, DMSO) δ 161.79, 159.03, 153.14, 144.64, 143.02, 136.60, 133.08, 131.84, 129.13, 128.88, 128.70, 127.53, 122.69, 121.20, 119.12, 113.45, 106.12. Anal. Calcd. for $C_{21}H_{13}N_5O_2$: C, 68.66; H, 3.57; N, 19.06. Found: C, 68.59; H, 3.80; N, 18.79.

N-(3-fluorophenyl)-6-nitro-2-phenylquinazolin-4-amine (21). The compound was synthesized according to the general procedure for compounds **14-42** from **8** (2.86 g, 10 mmol) and 3-fluoroaniline (1.11 g, 10 mmol) to yield **21** as a yellow solid (3.17 g, 88%), mp 288-289 °C (decomp.). ^{1}H NMR (500 MHz, DMSO-d_6) δ 11.10 (s, 1H), 9.73 (d, J = 2.5 Hz, 1H), 8.61 (dd, J = 9.2, 2.4 Hz, 1H), 8.51 – 8.36 (m, 2H), 8.18 (d, J = 9.2 Hz, 1H), 7.89 (dt, J = 11.4, 2.3 Hz, 1H), 7.75 (ddd, J = 8.2, 2.0, 0.9 Hz, 1H), 7.67 – 7.42 (m, 4H), 7.10 (tdd, J = 8.4, 2.5,

0.9 Hz, 1H). ^{13}C NMR (126 MHz, DMSO) δ 162.01 (d, *J* = 241.9 Hz), 161.25, 159.12, 144.76, 139.82 (d, *J* = 11.1 Hz), 135.45, 132.28, 130.31 (d, *J* = 9.4 Hz), 128.86, 127.86, 127.48, 121.23, 118.97, 113.18, 111.73 (d, *J* = 20.9 Hz), 110.12 (d, *J* = 26.0 Hz). Anal. Calcd. for $C_{20}H_{13}FN_4O_2$: C, 66.66; H, 3.64; N, 15.55. Found: C, 66.30; H, 3.92; N, 15.30.

6-nitro-2-phenyl-N-(3-(trifluoromethyl)phenyl)quinazolin-4-amine (22). The compound was synthesized according to the general procedure for compounds **14-42** from **8** (2.86 g, 10 mmol) and 3-(trifluoromethyl)aniline (1.61 g, 10 mmol) to yield **22** as a yellow solid (3.08 g, 75%), mp 278-279 °C (decomp.). ^{1}H NMR (600 MHz, DMSO-d_6) δ 10.65 (s, 1H), 9.65 (d, *J* = 2.4 Hz, 1H), 8.57 (d, *J* = 2.0 Hz, 1H), 8.54 (dd, *J* = 9.1, 2.4 Hz, 1H), 8.43 (dt, *J* = 7.1, 1.4 Hz, 2H), 8.20 – 8.13 (m, 1H), 7.98 (dd, *J* = 9.1, 1.8 Hz, 1H), 7.71 (t, *J* = 8.0 Hz, 1H), 7.59 – 7.53 (m, 2H), 7.53 – 7.47 (m, 2H). ^{13}C NMR (151 MHz, DMSO) δ 162.10, 158.99, 154.15, 144.44, 139.67, 137.40, 131.57, 129.91 (d, *J* = 5.2 Hz), 129.40 (d, *J* = 31.6 Hz), 128.71, 128.47, 127.13, 125.94, 124.44 (d, *J* = 272.5 Hz), 120.98, 120.55 (d, *J* = 3.7 Hz), 118.99 (d, *J* = 4.0 Hz), 113.37. Anal. Calcd. for $C_{21}H_{13}F_3N_4O_2$: C, 61.47; H, 3.19; N, 13.65. Found: C, 61.77; H, 3.35; N, 13.44.

2-nitro-4-((6-nitro-2-phenylquinazolin-4-yl)amino)phenol (23). The compound was synthesized according to the general procedure for compounds **14-42** from **8** (2.86 g, 10 mmol) and 4-amino-2-nitrophenol (1.54 g, 10 mmol) to yield **23** as an orange-red solid (2.58 g, 64%), mp >300 °C. ^{1}H NMR (500 MHz, DMSO-d_6) δ 10.90 (s, 1H), 10.56 (s, 1H), 9.61 (d, *J* = 2.5 Hz, 1H), 8.80 (d, *J* = 2.7 Hz, 1H), 8.54 (dd, *J* = 9.2, 2.4 Hz, 1H), 8.51 – 8.44 (m, 2H), 8.04 (dd, *J* = 9.0, 2.7 Hz, 1H), 7.98 (d, *J* = 9.2 Hz, 1H), 7.60 – 7.46 (m, 3H), 7.26 (d, *J* = 9.0 Hz, 1H). ^{13}C NMR (126 MHz, DMSO) δ 162.19, 158.80, 154.07, 149.22, 144.31, 137.40, 135.70, 131.45, 130.49, 130.16, 129.76, 128.67, 128.57, 127.00, 120.86, 119.39, 118.70, 113.25. Anal. Calcd. for $C_{20}H_{13}N_5O_5$: C, 59.56; H, 3.25; N, 17.36. Found: C, 59.69; H, 3.01; N, 17.22.

N-(3-((6-nitro-2-phenylquinazolin-4-yl)amino)phenyl)acetamide (24). The compound was synthesized according to the general procedure for compounds **14-42** from **8** (2.86 g, 10 mmol) and N-(3-aminophenyl)acetamide (1.50 g, 10 mmol) to yield **24** as a yellow solid (2.80 g, 70%), mp >300 °C. ^{1}H NMR (500 MHz, DMSO-d_6) δ 10.83 (s, 1H), 10.09 (s, 1H), 9.73 (d, J = 2.4 Hz, 1H), 8.60 (dd, J = 9.2, 2.5 Hz, 1H), 8.54 – 8.39 (m, 2H), 8.33 (t, J = 2.1 Hz, 1H), 8.08 (d, J = 9.2 Hz, 1H), 7.67 – 7.47 (m, 4H), 7.41 (t, J = 8.1 Hz, 1H), 7.31 (ddd, J = 8.0, 2.1, 1.0 Hz, 1H), 2.09 (s, 3H). ^{13}C NMR (126 MHz, DMSO) δ 168.54, 161.74, 159.20, 152.19, 144.58, 139.80, 138.46, 136.12, 131.93, 128.97, 128.76, 128.09, 127.54, 121.33, 118.20, 115.93, 114.17, 113.29, 24.18. Anal. Calcd. for $C_{22}H_{17}N_5O_3$: C, 66.16; H, 4.29; N, 17.53. Found: C, 66.26; H, 4.53; N, 17.25.

3-((6-nitro-2-phenylquinazolin-4-yl)amino)benzoic acid (25). The compound was synthesized according to the general procedure for compounds **14-42** from **8** (2.86 g, 10 mmol) and 3-aminobenzoic acid (1.37 g, 10 mmol) to yield **25** as a yellow solid (2.43 g, 63%), mp >300 °C. ^{1}H NMR (500 MHz, DMSO-d_6) δ 10.97 (s, 1H), 9.71 (d, J = 2.5 Hz, 1H), 8.58 (dd, J = 9.2, 2.4 Hz, 1H), 8.47 – 8.35 (m, 2H), 8.14 – 7.99 (m, 5H), 7.67 – 7.44 (m, 3H). ^{13}C NMR (126 MHz, DMSO) δ 167.01, 161.57, 159.04, 152.15, 144.67, 142.47, 136.04, 132.03, 130.16, 128.88, 128.83, 128.30, 127.63, 126.64, 122.28, 121.25, 113.35. Anal. Calcd. for $C_{21}H_{14}N_4O_4$: C, 65.28; H, 3.65; N, 14.50. Found: C, 65.58; H, 3.88; N, 14.29.

N-(3-methoxyphenyl)-6-nitro-2-(pyridin-3-yl)quinazolin-4-amine (26). The compound was synthesized according to the general procedure for compounds **14-42** from **9** (2.87 g, 10 mmol) and 3-methoxyaniline (1.23 g, 10 mmol) to yield **26** as a yellow solid (2.17 g, 58%), mp 268-269 °C (decomp.). ^{1}H NMR (500 MHz, DMSO-d_6) δ 10.38 (s, 1H), 9.56 (d, J = 2.5

Hz, 1H), 9.48 – 9.44 (m, 1H), 8.67 (dd, *J* = 4.7, 1.8 Hz, 1H), 8.59 (dt, *J* = 7.8, 2.0 Hz, 1H), 8.46 (dd, *J* = 9.0, 2.5 Hz, 1H), 7.88 (d, *J* = 9.1 Hz, 1H), 7.58 (t, *J* = 2.2 Hz, 1H), 7.52 – 7.42 (m, 2H), 7.35 (t, *J* = 8.1 Hz, 1H), 6.78 (ddd, *J* = 8.2, 2.5, 0.9 Hz, 1H), 3.81 (s, 3H). ^{13}C NMR (126 MHz, DMSO) δ 160.63, 159.49, 158.85, 153.77, 151.66, 149.59, 144.39, 139.70, 135.54, 132.91, 129.66, 129.34, 126.89, 123.69, 120.89, 114.95, 113.47, 110.43, 108.29, 55.29. Anal. Calcd. for $C_{20}H_{15}N_5O_3$: C, 64.34; H, 4.05; N, 18.76. Found: C, 64.26; H, 4.16; N, 19.10.

N-(4-methoxyphenyl)-6-nitro-2-(pyridin-3-yl)quinazolin-4-amine (27). The compound was synthesized according to the general procedure for compounds **14-42** from **9** (2.87 g, 10 mmol) and 4-methoxyaniline (1.23 g, 10 mmol) to yield **27** as a yellow solid (2.24 g, 60%), mp 269-270 °C (decomp.). ^{1}H NMR (500 MHz, DMSO-d_6) δ 10.54 (s, 1H), 9.50 (d, *J* = 2.6 Hz, 1H), 9.47 (dd, *J* = 2.1, 0.9 Hz, 1H), 8.66 (dd, *J* = 4.7, 1.7 Hz, 1H), 8.62 (dt, *J* = 7.9, 1.9 Hz, 1H), 8.42 (dd, *J* = 9.1, 2.5 Hz, 1H), 7.79 (d, *J* = 9.1 Hz, 1H), 7.75 – 7.68 (m, 2H), 7.50 (ddd, *J* = 7.9, 4.7, 0.9 Hz, 1H), 7.08 – 6.94 (m, 2H), 3.79 (s, 3H). ^{13}C NMR (126 MHz, DMSO) δ 161.04, 158.51, 155.77, 154.68, 151.32, 149.68, 143.63, 135.52, 133.70, 128.69, 126.37, 124.72, 123.61, 121.23, 115.36, 113.72, 55.38. Anal. Calcd. for $C_{20}H_{15}N_5O_3$: C, 64.34; H, 4.05; N, 18.76. Found: C, 64.48; H, 4.00; N, 18.39.

N-(4-methoxyphenyl)-6-nitro-2-(pyridin-4-yl)quinazolin-4-amine (28). The compound was synthesized according to the general procedure for compounds **14-42** from **10** (2.87 g, 10 mmol) and 4-methoxyaniline (1.23 g, 10 mmol) to yield **28** as an orange-red solid (2.31 g, 62%), mp 297-299 °C (decomp.). ^{1}H NMR (500 MHz, DMSO-d_6) δ 10.71 (s, 1H), 9.67 (d, *J* = 2.4 Hz, 1H), 9.02 – 8.84 (m, 2H), 8.61 – 8.48 (m, 3H), 8.03 (dd, *J* = 9.1, 1.2 Hz, 1H), 7.83 – 7.69 (m, 2H), 7.06 (dq, *J* = 9.4, 2.6, 1.8 Hz, 2H), 3.82 (s, 3H). ^{13}C NMR (126 MHz, DMSO) δ 159.30, 158.77, 156.69, 153.35, 150.11, 145.36, 145.24, 130.91, 129.98, 127.32, 124.79,

124.06, 121.01, 114.05, 113.97, 55.42. Anal. Calcd. for $C_{20}H_{15}N_5O_3$: C, 64.34; H, 4.05; N, 18.76. Found: C, 64.56; H, 4.27; N, 18.49.

3-((6-nitro-2-(pyridin-4-yl)quinazolin-4-yl)amino)benzonitrile (29). The compound was synthesized according to the general procedure for compounds **14-42** from **10** (2.87 g, 10 mmol) and 3-aminobenzonitrile (1.18 g, 10 mmol) to yield **29** as a yellow solid (2.65 g, 72%), mp >300 °C. ^{1}H NMR (500 MHz, DMSO-d_6) δ 10.97 (s, 1H), 9.67 (d, J = 2.4 Hz, 1H), 8.98 – 8.92 (m, 2H), 8.59 (dd, J = 9.2, 2.4 Hz, 1H), 8.55 – 8.49 (m, 2H), 8.28 (q, J = 1.4 Hz, 1H), 8.27 – 8.20 (m, 1H), 8.05 (d, J = 9.1 Hz, 1H), 7.72 – 7.67 (m, 2H). ^{13}C NMR (126 MHz, DMSO) δ 159.40, 158.49, 153.32, 149.88, 145.51, 145.40, 139.14, 130.33, 130.25, 128.34, 127.66, 126.09, 124.07, 121.03, 118.67, 114.02, 111.67. Anal. Calcd. for $C_{22}H_{14}N_6O_2$: C, 65.21; H, 3.28; N, 22.82. Found: C, 65.43; H, 3.49; N, 22.44.

6-nitro-N-phenyl-2-(3-(trifluoromethyl)phenyl)quinazolin-4-amine (30). The compound was synthesized according to the general procedure for compounds **14-42** from **11** (3.54 g, 10 mmol) and aniline (0.93 g, 10 mmol) to yield **30** as a yellow solid (3.08 g, 75%), mp 238-240 °C. ^{1}H NMR (500 MHz, DMSO-d_6) δ 10.56 (s, 1H), 9.63 (d, J = 2.5 Hz, 1H), 8.68 (dq, J = 1.4, 0.8 Hz, 1H), 8.64 (dd, J = 7.8, 1.6 Hz, 1H), 8.53 (dd, J = 9.2, 2.5 Hz, 1H), 7.98 (d, J = 9.2 Hz, 1H), 7.92 – 7.84 (m, 3H), 7.80 – 7.68 (m, 1H), 7.53 – 7.40 (m, 2H), 7.31 – 7.20 (m, 1H). ^{13}C NMR (126 MHz, DMSO) δ 160.63, 159.11, 153.96, 144.53, 138.52, 138.42, 132.01, 129.97, 129.79, 129.51 (d, J = 31.7 Hz), 129.13, 128.56, 127.66 (d, J = 3.3 Hz), 127.52, 127.03, 125.35, 124.86, 124.71 (d, J = 3.9 Hz), 123.13, 120.99, 113.55. Anal. Calcd. for $C_{21}H_{13}F_3N_4O_2$: C, 61.71; H, 3.29; N, 13.31. Found: C, 61.47; H, 3.19; N, 13.65.

3-((6-nitro-2-(3-(trifluoromethyl)phenyl)quinazolin-4-yl)amino)phenol (31). The compound was synthesized according to the general procedure for compounds **14-42** from **11**

(3.54 g, 10 mmol) and 3-aminophenol (1.09 g, 10 mmol) to yield **31** as a yellow solid (3.54 g, 83%), mp 275-278 °C (decomp.). ^{1}H NMR (500 MHz, DMSO-*d*6) δ 10.64 (s, 1H), 9.68 (d, *J* = 2.6 Hz, 1H), 8.55 (dd, *J* = 9.2, 2.4 Hz, 1H), 8.46 (ddd, *J* = 6.4, 3.1, 1.4 Hz, 2H), 8.20 – 8.09 (m, 2H), 8.11 – 8.03 (m, 2H), 8.00 (d, *J* = 9.2 Hz, 1H), 7.65 – 7.48 (m, 3H). ^{13}C NMR (126 MHz, DMSO) δ 165.49, 162.17, 158.92, 154.15, 144.43, 143.31, 137.35, 131.46, 130.01, 129.85, 128.80, 128.57, 127.10, 125.07, 121.73, 121.08, 113.46. Anal. Calcd. for $C_{21}H_{13}F_3N_4O_3$: C, 59.16; H, 3.07; N, 13.14. Found: C, 59.29; H, 3.30; N, 12.88.

N-(3-methoxyphenyl)-6-nitro-2-(3-(trifluoromethyl)phenyl)quinazolin-4-amine (32). The compound was synthesized according to the general procedure for compounds **14-42** from **11** (3.54 g, 10 mmol) and 3-methoxyaniline (1.23 g, 10 mmol) to yield **32** as a yellow solid (3.21 g, 73%), mp 207-209 °C. ^{1}H NMR (500 MHz, DMSO-d_6) δ 10.48 (s, 1H), 9.62 (d, *J* = 2.5 Hz, 1H), 8.71 – 8.63 (m, 2H), 8.52 (dd, *J* = 9.1, 2.5 Hz, 1H), 7.98 (d, *J* = 9.2 Hz, 1H), 7.92 – 7.85 (m, 1H), 7.75 (tt, *J* = 7.5, 0.8 Hz, 1H), 7.60 (t, *J* = 2.2 Hz, 1H), 7.47 (ddd, *J* = 8.0, 2.0, 0.9 Hz, 1H), 7.36 (t, *J* = 8.1 Hz, 1H), 6.81 (ddd, *J* = 8.2, 2.5, 0.9 Hz, 1H), 3.81 (s, 3H). ^{13}C NMR (126 MHz, DMSO) δ 160.63, 159.56, 159.06, 153.91, 144.56, 139.65, 138.57, 132.04, 129.94, 129.82, 129.55 (d, *J* = 31.8 Hz), 129.29, 129.17, 127.72, 127.69, 127.04, 125.35, 124.69, 124.66, 123.19, 120.96, 115.09, 113.59, 110.62, 108.51, 55.27. Anal. Calcd. for $C_{22}H_{15}F_3N_4O_3$: C, 60.00; H, 3.43; N, 12.72. Found: C, 59.99; H, 3.34; N, 12.34.

N-(3,4-dimethoxyphenyl)-6-nitro-2-(3-(trifluoromethyl)phenyl)quinazolin-4-amine (33). The compound was synthesized according to the general procedure for compounds **14-42** from **11** (3.54 g, 10 mmol) and 3,4-dimethoxyaniline (1.53 g, 10 mmol) to yield **33** as a red solid (2.78 g, 59%), mp 217-218 °C. ^{1}H NMR (500 MHz, DMSO-d_6) δ 10.45 (s, 1H), 9.59 (d, *J* = 2.4 Hz, 1H), 8.69 – 8.59 (m, 2H), 8.50 (dd, *J* = 9.2, 2.5 Hz, 1H), 7.95 (d, *J* = 9.2 Hz, 1H), 7.92 – 7.83 (m, 1H), 7.78 – 7.70 (m, 1H), 7.60 (d, *J* = 2.4 Hz, 1H), 7.35 (dd, *J* = 8.6, 2.5 Hz,

1H), 7.02 (d, *J* = 8.7 Hz, 1H), 3.81 (s, 3H), 3.80 (s, 3H). ^{13}C NMR (126 MHz, DMSO) δ 160.66, 158.88, 153.68, 148.51, 146.22, 144.45, 138.56, 132.09, 131.62, 129.89, 129.53, 129.47 (d, *J* = 31.8 Hz), 127.69, 127.66, 127.52, 126.96, 124.59 (d, *J* = 3.7 Hz), 124.28 (d, *J* = 272.4 Hz), 120.87, 115.10, 113.52, 111.70, 107.98, 55.88, 55.60. Anal. Calcd. for $C_{23}H_{17}F_3N_4O_4$: C, 58.73; H, 3.64; N, 11.91. Found: C, 58.53; H, 3.63; N, 11.58.

N-(3-(Methylthio)phenyl)-6-nitro-2-(3-(trifluoromethyl)phenyl)quinazolin-4-amine (34). The compound was synthesized according to the general procedure for compounds **14-42** from **11** (3.54 g, 10 mmol) and 3-(methylthio)aniline (1.39 g, 10 mmol) to yield **34** as a orange solid (3.56 g, 78%), mp 209-211 °C. ^{1}H NMR (600 MHz, DMSO-d_6) δ 10.48 (s, 1H), 9.58 (d, *J* = 2.5 Hz, 1H), 8.68 – 8.61 (m, 2H), 8.50 (dd, *J* = 9.1, 2.4 Hz, 1H), 7.96 (d, *J* = 9.1 Hz, 1H), 7.90 – 7.83 (m, 2H), 7.76 – 7.70 (m, 1H), 7.66 (ddd, *J* = 8.1, 2.1, 0.9 Hz, 1H), 7.39 (t, *J* = 7.9 Hz, 1H), 7.12 (ddd, *J* = 7.9, 1.9, 0.9 Hz, 1H), 2.51 (s, 3H). ^{13}C NMR (151 MHz, DMSO) δ 160.55, 159.03, 153.87, 144.53, 139.01, 138.64, 138.49, 132.06, 129.89, 129.82, 129.56 (d, *J* = 31.8 Hz), 129.03, 127.76, 127.05, 125.16, 124.61 (d, *J* = 4.0 Hz), 123.35, 122.17, 120.91, 120.12, 119.36, 113.54, 14.94. Anal. Calcd. for $C_{22}H_{15}F_3N_4O_2S$: C, 57.89; H, 3.31; N, 12.27. Found: C, 57.99; H, 3.25; N, 12.03.

N-(3-Fluorophenyl)-6-nitro-2-(3-(trifluoromethyl)phenyl)quinazolin-4-amine (35). The compound was synthesized according to the general procedure for compounds **14-42** from **11** (3.54 g, 10 mmol) and 3-fluoroaniline (1.11 g, 10 mmol) to yield **35** as a yellow solid (3.47 g, 81%), mp 238-239 °C. ^{1}H NMR (500 MHz, DMSO-d_6) δ 10.52 (s, 1H), 9.54 (d, *J* = 2.5 Hz, 1H), 8.61 (td, *J* = 1.7, 0.8 Hz, 1H), 8.59 (dd, *J* = 7.8, 1.5 Hz, 1H), 8.48 (dd, *J* = 9.1, 2.5 Hz, 1H), 7.98 – 7.82 (m, 3H), 7.77 – 7.68 (m, 1H), 7.65 (ddd, *J* = 8.1, 2.0, 0.9 Hz, 1H), 7.46 (td, *J* = 8.2, 6.8 Hz, 1H), 7.04 (tdd, *J* = 8.4, 2.6, 0.8 Hz, 1H). ^{13}C NMR (126 MHz, DMSO) δ

163.02, 161.10, 160.41, 158.86, 153.76, 144.55, 140.25 (d, J = 11.0 Hz), 138.30, 131.89, 130.08, 130.01, 129.92, 129.84, 129.67, 129.42, 129.16, 127.72, 127.69, 127.47, 127.04, 125.30, 124.65 (d, J = 3.9 Hz), 123.14, 120.81, 118.32 (d, J = 2.3 Hz), 113.43, 111.05 (d, J = 21.0 Hz), 109.62 (d, J = 26.2 Hz). Anal. Calcd. for $C_{21}H_{12}F_4N_4O_2$: C, 58.88; H, 2.82; N, 13.08. Found: C, 58.91; H, 2.73; N, 12.81.

6-Nitro-N-(3-nitrophenyl)-2-(3-(trifluoromethyl)phenyl)quinazolin-4-amine (36). The compound was synthesized according to the general procedure for compounds **14-42** from **11** (3.54 g, 10 mmol) and 3-nitroaniline (1.38 g, 10 mmol) to yield **36** as a yellow solid (3.92 g, 86%), mp 278-279 °C. ^{1}H NMR (500 MHz, DMSO-d_6) δ 10.87 (s, 1H), 9.69 (s, 1H), 9.10 (d, J = 2.6 Hz, 1H), 8.74 (d, J = 16.3 Hz, 2H), 8.63 – 8.56 (m, 1H), 8.30 (d, J = 8.2 Hz, 1H), 8.08 (t, J = 8.1 Hz, 2H), 7.93 (d, J = 8.0 Hz, 1H), 7.77 (q, J = 8.2 Hz, 2H). ^{13}C NMR (126 MHz, DMSO) δ 160.46, 159.11, 153.84, 147.92, 144.79, 138.27, 132.17, 130.07, 129.98, 128.39, 127.89, 127.35, 124.65, 120.93, 118.85, 116.87. Anal. Calcd. for $C_{21}H_{12}F_3N_5O_4$: C, 55.39; H, 2.66; N, 15.38. Found: C, 55.35; H, 2.61; N, 15.08.

6-Nitro-N-(4-nitrophenyl)-2-(3-(trifluoromethyl)phenyl)quinazolin-4-amine (37). The compound was synthesized according to the general procedure for compounds **14-42** from **11** (3.54 g, 10 mmol) and 4-nitroaniline (1.38 g, 10 mmol) to yield **37** as a bright yellow solid (3.23 g, 71%), mp > 300 °C. ^{1}H NMR (500 MHz, DMSO-d_6) δ 10.86 (s, 1H), 9.63 (d, J = 2.4 Hz, 1H), 8.68 (s, 1H), 8.66 (d, J = 7.9 Hz, 1H), 8.57 (dd, J = 9.1, 2.5 Hz, 1H), 8.36 – 8.30 (m, 2H), 8.25 – 8.19 (m, 2H), 8.05 (d, J = 9.2 Hz, 1H), 7.91 (d, J = 7.7 Hz, 1H), 7.80 (q, J = 8.3, 7.8 Hz, 1H). ^{13}C NMR (126 MHz, DMSO) δ 160.41, 158.98, 153.87, 145.14, 144.84, 142.85, 138.11, 132.24, 130.25, 130.09, 129.73, 129.48, 127.92, 127.89, 127.41, 124.69, 124.66, 124.54, 123.17, 122.09, 121.00, 120.32, 120.27, 113.76. Anal. Calcd. for $C_{21}H_{12}F_3N_5O_4$: C, 55.39; H, 2.66; N, 15.38. Found: C, 55.42; H, 2.67; N, 15.12.

2-Nitro-4-((6-nitro-2-(3-(trifluoromethyl)phenyl)quinazolin-4-yl)amino)phenol (38). The compound was synthesized according to the general procedure for compounds **14-42** from **11** (3.54 g, 10 mmol) and 4-amino-2-nitrophenol (1.54 g, 10 mmol) to yield **38** as a yellow solid (3.25 g, 69%), mp 280-281 °C (decomp.). ^{1}H NMR (500 MHz, DMSO-d_6) δ 10.89 (s, 1H), 10.50 (s, 1H), 9.49 (d, J = 2.5 Hz, 1H), 8.66 – 8.57 (m, 3H), 8.46 (dd, J = 9.1, 2.4 Hz, 1H), 7.97 (dd, J = 9.0, 2.7 Hz, 1H), 7.91 (d, J = 9.1 Hz, 1H), 7.85 (ddt, J = 7.7, 1.9, 1.0 Hz, 1H), 7.73 – 7.66 (m, 1H), 7.20 (d, J = 9.0 Hz, 1H). ^{13}C NMR (126 MHz, DMSO) δ 160.45, 158.71, 153.68, 149.33, 144.48, 138.27, 135.57, 132.08, 130.15, 130.12, 129.81 (d, J = 3.5 Hz), 129.67, 129.41, 127.71, 127.69, 126.98, 124.61, 124.58, 124.21 (d, J = 272.4 Hz), 120.69, 119.19, 118.72, 113.34. Anal. Calcd. for $C_{21}H_{12}F_3N_5O_5$: C, 53.51; H, 2.57; N, 14.86. Found: C, 53.75; H, 2.61; N, 14.59.

N-(3-((6-Nitro-2-(3-(trifluoromethyl)phenyl)quinazolin-4-yl)amino)phenyl)acetamide (39). The compound was synthesized according to the general procedure for compounds **14-42** from **11** (3.54 g, 10 mmol) and N-(3-aminophenyl)acetamide (1.50 g, 10 mmol) to yield **39** as a yellow solid (2.85 g, 61%), mp > 300 °C. ^{1}H NMR (500 MHz, DMSO-d_6) δ 10.63 (s, 1H), 10.04 (s, 1H), 9.68 (d, J = 2.5 Hz, 1H), 8.80 – 8.63 (m, 2H), 8.55 (dd, J = 9.2, 2.5 Hz, 1H), 8.43 (t, J = 2.1 Hz, 1H), 8.01 (d, J = 9.1 Hz, 1H), 7.89 (dd, J = 7.9, 1.5 Hz, 1H), 7.75 (t, J = 7.8 Hz, 1H), 7.53 (ddd, J = 8.0, 2.2, 1.1 Hz, 1H), 7.37 (t, J = 8.0 Hz, 1H), 7.29 (ddd, J = 8.0, 2.1, 1.1 Hz, 1H), 2.07 (s, 3H). ^{13}C NMR (126 MHz, DMSO) δ 168.46, 160.66, 159.16, 153.79, 144.58, 139.76, 138.62, 138.32, 132.32, 129.91, 129.62, 129.39, 129.14, 128.55, 127.75, 127.73, 127.12, 125.02, 124.99, 124.28 (d, J = 272.3 Hz), 121.14, 117.85, 115.55, 114.05, 113.58, 24.10. Anal. Calcd. for $C_{23}H_{16}F_3N_5O_3$: C, 59.10; H, 3.45; N, 14.98. Found: C, 59.42; H, 3.59; N, 14.73.

4-((2-(3-Methoxyphenyl)-6-nitroquinazolin-4-yl)amino)benzonitrile (40). The compound was synthesized according to the general procedure for compounds **14-42** from **12** (3.16 g, 10 mmol) and 4-aminobenzonitrile (1.18 g, 10 mmol) to yield **40** as a yellow solid (2.34 g, 59%), mp 184-186 °C. ^{1}H NMR (500 MHz, DMSO-d_6) δ 10.63 (s, 1H), 9.56 (d, J = 2.4 Hz, 1H), 8.50 (dt, J = 9.0, 2.8 Hz, 1H), 8.20 – 8.11 (m, 2H), 7.99 – 7.92 (m, 2H), 7.91 – 7.87 (m, 3H), 7.40 (t, J = 7.9 Hz, 1H), 7.09 (ddd, J = 8.2, 2.7, 0.9 Hz, 1H), 3.83 (s, 3H). ^{13}C NMR (126 MHz, DMSO) δ 161.71, 159.53, 158.73, 154.03, 144.44, 143.21, 138.64, 132.93, 129.90, 129.81, 127.11, 122.36, 120.96, 120.91, 119.15, 117.66, 113.42, 113.05, 105.82, 55.20. Anal. Calcd. for $C_{22}H_{15}N_5O_3$: C, 66.49; H, 3.80; N, 17.62. Found: C, 66.24; H, 4.00; N, 17.33.

N-(3-Fluorophenyl)-2-(3-methoxyphenyl)-6-nitroquinazolin-4-amine (41). The compound was synthesized according to the general procedure for compounds **14-42** from **12** (3.16 g, 10 mmol) and 3-fluoroaniline (1.11 g, 10 mmol) to yield **41** as a yellow-orange solid (3.44 g, 88%), mp 276-277 °C (decomp.). ^{1}H NMR (500 MHz, DMSO-d_6) δ 10.51 (s, 1H), 9.61 (d, J = 2.5 Hz, 1H), 8.51 (dd, J = 9.2, 2.5 Hz, 1H), 8.05 – 7.91 (m, 4H), 7.71 (ddd, J = 8.3, 2.0, 0.9 Hz, 1H), 7.49 (td, J = 8.3, 6.9 Hz, 1H), 7.42 (t, J = 7.9 Hz, 1H), 7.10 (ddd, J = 8.2, 2.8, 1.0 Hz, 1H), 7.03 (tdd, J = 8.4, 2.6, 0.9 Hz, 1H), 3.83 (s, 3H). ^{13}C NMR (126 MHz, DMSO) δ 162.07 (d, J = 241.3 Hz), 161.84, 159.53, 158.80, 154.04, 144.34, 140.53 (d, J = 11.1 Hz), 138.88, 130.13 (d, J = 9.4 Hz), 129.81, 129.74, 126.96, 120.91, 120.82, 118.26, 118.24, 117.70, 113.32, 112.96, 110.83 (d, J = 21.1 Hz), 109.47 (d, J = 26.2 Hz), 55.08. Anal. Calcd. for $C_{21}H_{15}FN_4O_3$: C, 64.61; H, 3.87; N, 14.35. Found: C, 64.84; H, 3.93; N, 14.23.

2-(3,4-Dimethoxyphenyl)-6-nitro-N-(3-(trifluoromethyl)phenyl)quinazolin-4-amine (42). The compound was synthesized according to the general procedure for compounds **14-42** from **13** (3.46 g, 10 mmol) and 3-(trifluoromethyl)aniline (1.61 g, 10 mmol) to yield **42** as a orange solid (3.39 g, 72%), mp >300 °C. ^{1}H NMR (600 MHz, DMSO-d_6) δ 10.63 (s, 1H),

9.64 (d, *J* = 2.4 Hz, 1H), 8.54 (dd, *J* = 9.2, 2.4 Hz, 1H), 8.41 (d, *J* = 2.0 Hz, 1H), 8.31 – 8.23 (m, 1H), 8.07 (dd, *J* = 8.4, 2.0 Hz, 1H), 8.01 (d, *J* = 2.0 Hz, 1H), 7.97 (d, *J* = 9.1 Hz, 1H), 7.72 (t, *J* = 8.0 Hz, 1H), 7.55 (d, *J* = 7.9 Hz, 1H), 7.08 (d, *J* = 8.5 Hz, 1H), 3.85 (s, 3H), 3.84 (s, 3H). ^{13}C NMR (126 MHz, DMSO) δ 161.85, 158.65, 154.21, 152.00, 148.67, 143.93, 139.69, 129.79, 129.74, 129.51, 126.94, 126.09, 125.46, 123.29, 122.15, 120.91, 120.49 (d, *J* = 3.5 Hz), 118.73 (d, *J* = 3.8 Hz), 112.94, 111.36, 55.74, 55.38. Anal. Calcd. for $C_{23}H_{17}F_3N_4O_4$: C, 58.73; H, 3.64; N, 11.91. Found: C, 58.79; H, 3.92; N, 11.65.

General Procedure for the Preparation of compounds 43-47. The corresponding 2- and 4-substituted 6-nitroquinazoline derivative (1 mmol) was dissolved in dry THF (200 mL) and added to a pressure vessel together with 1% (by weight of the educt) of Pd activated charcoal. After evacuating and flushing the vessel with N_2 three times, it was pressurized with hydrogen gas (4 bar) and sealed. The mixture was stirred for 24 h at room temperature until completion of the reaction as indicated by TLC. Charcoal was removed by several filtration cycles and the remaining solvent evaporated under reduced pressure to obtain the corresponding compound as a solid product. Purification was carried out by column chromatography using DCM and methanol as eluent.

N4-(3-Methoxyphenyl)-2-(pyridin-3-yl)quinazoline-4,6-diamine (43). The compound was synthesized according to the general procedure for compounds **43-47** from **26** (3.73 g, 10 mmol) to yield **43** as a yellow solid (1.65 g, 45%), mp 209-211 °C. ^{1}H NMR (500 MHz, DMSO-d_6) δ 9.50 (dd, *J* = 2.1, 0.9 Hz, 1H), 9.44 (s, 1H), 8.68 – 8.57 (m, 2H), 7.72 (t, *J* = 2.3 Hz, 1H), 7.64 (d, *J* = 8.8 Hz, 1H), 7.56 – 7.52 (m, 1H), 7.49 (ddd, *J* = 7.9, 4.8, 0.9 Hz, 1H), 7.41 (d, *J* = 2.4 Hz, 1H), 7.33 (d, *J* = 8.2 Hz, 1H), 7.31 – 7.25 (m, 1H), 6.69 (ddd, *J* = 8.2, 2.5, 0.9 Hz, 1H), 5.65 (s, 2H), 3.81 (s, 3H). ^{13}C NMR (126 MHz, DMSO) δ 159.53, 156.25, 152.87, 150.10, 148.73, 147.73, 143.12, 141.26, 134.36, 134.31, 129.28, 125.01, 124.04,

123.60, 115.91, 113.89, 108.86, 107.15, 101.49, 55.17. Anal. Calcd. for $C_{20}H_{17}N_5O$: C, 69.96; H, 4.99; N, 20.40. Found: C, 69.83; H, 5.21; N, 20.47.

N4-(4-Methoxyphenyl)-2-(pyridin-3-yl)quinazoline-4,6-diamine (44). The compound was synthesized according to the general procedure for compounds **43-47** from **27** (3.73 g, 10 mmol) to yield **44** as a yellow solid (2.13 g, 62%), mp 202-203 °C. ^{1}H NMR (500 MHz, DMSO-d_6) δ 9.45 (d, J = 2.1 Hz, 1H), 9.39 (s, 1H), 8.63 – 8.54 (m, 2H), 7.86 – 7.75 (m, 2H), 7.60 (d, J = 8.8 Hz, 1H), 7.47 (dd, J = 7.8, 4.8 Hz, 1H), 7.40 (d, J = 2.4 Hz, 1H), 7.25 (dd, J = 8.9, 2.2 Hz, 1H), 7.07 – 6.95 (m, 2H), 5.60 (s, 2H), 3.79 (s, 3H). ^{13}C NMR (126 MHz, DMSO) δ 156.46, 155.47, 153.04, 149.97, 148.75, 147.55, 142.90, 139.28, 134.36, 132.88, 129.15, 125.01, 123.69, 123.54, 115.72, 113.74, 101.63, 55.36. Anal. Calcd. for $C_{20}H_{17}N_5O$: C, 69.96; H, 4.99; N, 20.40. Found: C, 70.16; H, 5.32; N, 20.56.

N4-Phenyl-2-(3-(trifluoromethyl)phenyl)quinazoline-4,6-diamine (45). The compound was synthesized according to the general procedure for compounds **43-47** from **30** (4.10 g, 10 mmol) to yield **45** as a beige solid (2.40 g, 63%), mp 191-192 °C. ^{1}H NMR (500 MHz, DMSO-d_6) δ 9.50 (s, 1H), 8.67 (d, J = 1.7 Hz, 1H), 8.62 (dd, J = 7.8, 1.5 Hz, 1H), 7.96 – 7.90 (m, 2H), 7.80 – 7.74 (m, 1H), 7.75 – 7.68 (m, 1H), 7.66 (d, J = 8.8 Hz, 1H), 7.45 – 7.37 (m, 3H), 7.28 (dd, J = 8.9, 2.3 Hz, 1H), 7.12 (tt, J = 7.4, 1.2 Hz, 1H), 5.66 (s, 2H). ^{13}C NMR (126 MHz, DMSO) δ 156.36, 153.02, 147.79, 143.11, 140.02, 139.96, 130.84, 129.71, 129.35 (d, J = 31.5 Hz), 129.35, 128.42, 125.77 (d, J = 3.5 Hz), 125.58, 124.05, 123.57 (d, J = 3.8 Hz), 123.25, 122.00, 115.90, 101.52. Anal. Calcd. for $C_{21}H_{15}F_3N_4$: C, 66.31; H, 3.98; N, 14.73. Found: C, 66.42; H, 4.07; N, 14.45.

3-((6-Amino-2-(3-(trifluoromethyl)phenyl)quinazolin-4-yl)amino)phenol (46). The compound was synthesized according to the general procedure for compounds **43-47** from **31**

(4.26 g, 10 mmol) to yield **46** as a yellow solid (2.89 g, 73%), mp 190-192 °C. ^{1}H NMR (500 MHz, DMSO-d_6) δ 9.72 (s, 1H), 8.42 – 8.36 (m, 2H), 8.21 – 8.13 (m, 2H), 8.04 – 7.99 (m, 2H), 7.65 (d, J = 8.9 Hz, 1H), 7.54 – 7.47 (m, 2H), 7.47 – 7.38 (m, 2H), 7.30 (dd, J = 8.9, 2.4 Hz, 1H), 5.66 (s, 2H). ^{13}C NMR (126 MHz, DMSO) δ 165.65, 155.88, 154.46, 147.57, 144.96, 143.68, 138.77, 130.03, 129.50, 129.30, 128.53, 127.34, 124.37, 123.37, 120.23, 115.87, 101.34. Anal. Calcd. for $C_{21}H_{15}F_3N_4O$: C, 63.63; H, 3.81; N, 14.14. Found: C, 63.49; H, 4.14; N, 14.08.

N4-(3-Methoxyphenyl)-2-(3-(trifluoromethyl)phenyl)quinazoline-4,6-diamine (47). The compound was synthesized according to the general procedure for compounds **43-47** from **32** (4.40 g, 10 mmol) to yield **47** as a beige solid (2.42 g, 59%), mp 203-205 °C. ^{1}H NMR (500 MHz, DMSO-d_6) δ 9.46 (s, 1H), 8.71 – 8.61 (m, 2H), 7.81 – 7.75 (m, 1H), 7.74 – 7.68 (m, 2H), 7.66 (d, J = 8.9 Hz, 1H), 7.50 (ddd, J = 8.1, 2.0, 0.9 Hz, 1H), 7.41 (d, J = 2.4 Hz, 1H), 7.33 – 7.26 (m, 2H), 6.69 (ddd, J = 8.2, 2.5, 0.9 Hz, 1H), 5.67 (s, 2H), 3.80 (s, 3H). ^{13}C NMR (126 MHz, DMSO) δ 159.54, 156.27, 152.97, 147.80, 143.08, 141.20, 140.04, 130.86, 129.65, 129.50, 129.35, 129.24, 129.10, 127.71, 125.80, 125.55, 124.07, 123.50, 123.38, 115.95, 113.95, 108.99, 107.22, 101.46, 55.11. Anal. Calcd. for $C_{22}H_{17}F_3N_4O$: C, 64.39; H, 4.18; N, 13.65. Found: C, 64.32; H, 4.29; N, 13.40.

General Procedure for the Preparation of compounds 48-51.

The corresponding 6-amino-derivative **43** or **44** (10 mmol) was dissolved in a solution of 20 mL TAM in 80 mL THF under nitrogen in a Schlenk flask. The temperature was adjusted with a cooling bath to 0 °C and a solution of two (20 mmol) or one equivalent (10 mmol) of the corresponding acid chloride in THF added drop wise, respectively. After 30 min the cooling bath was removed and the solution was stirred for further 6-12 h. Completion of the reaction was monitored by TLC and the excess THF removed under reduced pressure. Water

was added to the mixture until precipitation of the product was visible. The formed precipitate was then filtered with suction and washed thoroughly with water. Recrystallization of the product was carried out with MeOH/H_2O to yield compounds **48-51**.

(E)-Acetic (E)-N-(4-((3-methoxyphenyl)amino)-2-(pyridin-3-yl)quinazolin-6-yl)acetimidic anhydride (48). The compound was synthesized according to the general procedure for compounds **48-51** from **43** (4.28 g, 10 mmol) and acetyl chloride (0.78 g, 20 mmol) to yield **48** as a beige-white solid (3.16 g, 74%), mp 242-244 °C. ^{1}H NMR (500 MHz, DMSO-d_6) δ 10.50 (s, 1H), 9.56 (s, 1H), 8.77 – 8.67 (m, 2H), 8.60 (d, J = 2.3 Hz, 1H), 8.17 – 8.08 (m, 2H), 7.58 (dd, J = 7.7, 5.0 Hz, 1H), 7.52 – 7.46 (m, 2H), 7.04 – 6.96 (m, 2H), 3.74 (s, 3H), 2.15 (s, 3H), 2.10 (s, 3H). ^{13}C NMR (126 MHz, DMSO) δ 170.67, 169.36, 162.31, 158.82, 156.77, 151.46, 149.33, 149.09, 139.44, 135.17, 133.36, 132.55, 129.45, 128.62, 124.03, 120.74, 114.87, 111.37, 55.49, 24.32, 22.98. Anal. Calcd. for $C_{24}H_{21}N_5O_3$: C, 67.44; H, 4.95; N; 16.38. Found: C, 67.72; H, 5.20; N; 16.07.

N-(4-((3-Methoxyphenyl)amino)-2-(pyridin-3-yl)quinazolin-6-yl)-3-nitrobenzamide (49). The compound was synthesized according to the general procedure for compounds **48-51** from **43** (4.28 g, 10 mmol) and 3-nitrobenzoyl chloride (1.86 g, 10 mmol) to yield **49** as a beige-white solid (3.99 g, 81%), mp >300 °C. ^{1}H NMR (500 MHz, DMSO-d_6) δ 10.97 (s, 1H), 9.97 (s, 1H), 9.55 (d, J = 1.9 Hz, 1H), 8.98 – 8.84 (m, 2H), 8.68 (td, J = 6.9, 5.8, 1.9 Hz, 2H), 8.56 – 8.42 (m, 2H), 8.10 (dd, J = 8.9, 2.2 Hz, 1H), 7.94 (d, J = 8.8 Hz, 1H), 7.89 (t, J = 8.0 Hz, 1H), 7.67 (t, J = 2.3 Hz, 1H), 7.59 – 7.50 (m, 2H), 7.36 (t, J = 8.1 Hz, 1H), 6.75 (dd, J = 8.3, 2.5 Hz, 1H), 3.82 (s, 3H). ^{13}C NMR (126 MHz, DMSO) δ 163.56, 159.52, 157.89, 156.81, 150.94, 149.21, 148.00, 147.77, 140.64, 136.43, 135.92, 135.00, 134.30, 133.77, 130.53, 129.31, 128.78, 128.76, 126.57, 123.71, 122.51, 114.55, 114.51, 109.63, 107.84, 55.22. Anal. Calcd. for $C_{27}H_{20}N_6O_4$: C, 65.85; H, 4.09; N; 17.06. Found: C, 65.73; H, 4.37 N; 17.03.

N-(4-((4-Methoxyphenyl)amino)-2-(pyridin-3-yl)quinazolin-6-yl)-3-nitrobenzamide (50). The compound was synthesized according to the general procedure for compounds **48-51** from **44** (4.28 g, 10 mmol) and 3-nitrobenzoyl chloride (1.86 g, 10 mmol) to yield **50** as a yellow solid (3.35 g, 68%), mp >300 °C. ^{1}H NMR (500 MHz, DMSO-d_6) δ 11.03 (s, 1H), 9.96 (s, 1H), 9.50 (d, J = 2.1 Hz, 1H), 8.93 (s, 1H), 8.90 (s, 1H), 8.67 – 8.62 (m, 2H), 8.51 (s, 1H), 8.48 (d, J = 8.2 Hz, 1H), 8.09 (d, J = 8.9 Hz, 1H), 7.90 (d, J = 8.7 Hz, 2H), 7.81 (d, J = 8.4 Hz, 2H), 7.55 – 7.48 (m, 1H), 7.04 (d, J = 8.5 Hz, 2H), 3.80 (s, 3H). ^{13}C NMR (126 MHz, DMSO) δ 163.51, 158.01, 156.92, 155.93, 150.81, 149.22, 148.00, 147.62, 136.30, 135.96, 135.01, 134.31, 133.85, 132.24, 130.49, 128.63, 128.50, 126.53, 124.30, 123.66, 122.55, 114.57, 114.37, 113.79, 55.38. Anal. Calcd. for $C_{27}H_{20}N_6O_4$: C, 65.85; H, 4.09; N, 17.06. Found: C, 65.61; H, 4.44; N, 16.77.

N-(4-((3-Methoxyphenyl)amino)-2-(pyridin-3-yl)quinazolin-6-yl)-3-nitrobenzamide (51). The compound was synthesized according to the general procedure for compounds **48-51** from **43** (4.28 g, 10 mmol) and nicotinoyl chloride (1.42 g, 10 mmol) to yield **51** as a yellow solid (2.56 g, 57%), mp 204-206 °C. ^{1}H NMR (500 MHz, DMSO-d_6) δ 9.96 (s, 1H), 9.55 (d, J = 2.0 Hz, 1H), 9.21 (d, J = 2.3 Hz, 1H), 8.94 (d, J = 2.2 Hz, 1H), 8.80 (dd, J = 4.8, 1.5 Hz, 1H), 8.75 – 8.65 (m, 2H), 8.39 (dt, J = 7.8, 2.1 Hz, 1H), 8.05 (dd, J = 8.9, 2.2 Hz, 1H), 7.93 (d, J = 8.9 Hz, 1H), 7.67 (t, J = 2.3 Hz, 1H), 7.62 (ddd, J = 7.9, 4.8, 0.9 Hz, 1H), 7.58 – 7.51 (m, 2H), 7.36 (t, J = 8.1 Hz, 1H), 6.80 – 6.70 (m, 1H), 3.82 (d, J = 0.8 Hz, 3H). ^{13}C NMR (126 MHz, DMSO) δ 164.29, 159.54, 157.90, 156.75, 152.53, 150.94, 149.22, 148.86, 147.70, 140.69, 136.59, 135.59, 135.00, 133.80, 130.26, 129.31, 128.79, 128.64, 123.78, 123.73, 114.58, 114.55, 114.25, 109.63, 107.86, 55.24. Anal. Calcd. for $C_{26}H_{20}N_6O_2$: C, 69.63; H, 4.50; N, 18.74. Found: C, 69.91; H, 4.77; N, 18.36.

Biological investigations. Materials for biological investigation. All chemicals were purchased from Sigma-Aldrich (Taufkirchen, Germany) besides compound **59** (Ko143) ((3S,6S,12aS)-1,2,3,4,6,7,12,12a-Octahydro-9-methoxy-6-(2-methylpropyl)-1,4-dioxopyrazino[1′,2′:1,6]pyrido[3,4-b]indole-3-propanoicacid1,1-dimethylethyl ester), which was purchased from Tocris Bioscience (Bristol, United Kingdom).

All assays performed with cells were carried out with 10 mM stock solutions of the test compound in DMSO. Krebs-HEPES buffer (KHB) was prepared from a solution of 118.6 mM NaCl, 4.7 mM KCl, 1.2 mM $MgSO_4$, 2.5 mM CaCl, 11.7 mM D-glucose monohydrate with addition of 10.0 mM HEPES in doubly distilled water. The pH of the solution was adjusted by an aqueous 4 N NaOH solution at 37 °C and sterilized, using a 0.2 µM membrane filter.

Cell culture. MDCK II BCRP cells were generated by transfection of the canine kidney epithelial cell line MDCK II with human wild-type cDNA C-terminally linked to the cDNA of the green fluorescent protein (GFP) and were a kind gift of Dr. A. Schinkel (The Netherlands Cancer Institute, Amsterdam, The Netherlands). Culturing of those cells was carried out with Dulbecco's modified Eagle's medium (DMEM) containing 10% fetal calf serum (FCS), 50 µg/mL streptomycin, 50 U/mL penicillin G and 2 mM *L*-glutamine. Furthermore, the human ovarian carcinoma cell line A2780adr was purchased from European Collection of Animal Cell Culture (ECACC, No 93112520) with an overexpression of P-gp and resistance against doxorubicin. For culturing RPMI-1640 medium supplemented with 20% FCS, 50 µg/mL streptomycin, 50 U/mL penicillin G and 2 mM *L*-glutamine was used. By treatment with doxorubicin every 10 passages for less than 40 passages the overexpression of P-gp was sustained. Moreover, small cell lung cancer cell line H69AR with overexpression of MRP1 was purchased from American Type Culture Collection (ATCC, CRL-11351). Culture of the cells was performed in RPMI 1640 medium enriched with 20% FCS, 50 mg/mL streptomycin, 50 U/mL penicillin G and 2 mM *L*-glutamine and stored under a 5%

CO_2 humidified atmosphere at 37 °C. Cells were harvested at a confluence of 80-90% and the subculturing of cells performed with 0.05% Trypsin and 0.02% EDTA. To remove excess medium cell were washed with PBS prior to trypsination. The detached cells were collected with medium and centrifuged in a 50 mL falcon (266 x g, 4 °C, 4 min). Excess liquid was removed by suction followed by resuspension of the obtained cell pellet in fresh medium. Measurement of the cell density for all cells was carried out with a CASY1 model TT cell counter equipped with a 150 µm capillary (Schaerfe System GmbH, Reutlingen, Germany). Before using the cells in the corresponding assay, they were washed with KHB three times. Myeloid leukemia cell line PLB-985 was cultured in RPMI 1640 medium with 10% FCS, 50 mg/mL streptomycin, 50 U/mL penicillin G and 2 mM *L*-glutamine under a 5% CO_2 humidified atmosphere at 37 °C. The suspension cells were harvested by centrifugation in a 50 mL falcon at (266 x g, 4 °C, 4 min) obtaining a cell pellet. Preparation for the cell based assay was carried out accordingly as described for the other cell lines above.

Hoechst 33342 accumulation assay. In the Hoechst 33342 accumulation assay the inhibitory effect on ABCG2 was determined for all test compounds with small modifications, described earlier in literature. [42,43,54,45,46,47,48,49,50,51,52,53,57] Test compounds were dissolved in DMSO to yield stock solutions of a concentration of 10 mM. Dilution series were performed with the corresponding stock solution together with sterile filtered KHB.

Cells were detached at a confluence of 80-90% by gentle trypsination (0.05% trypsin/0.02% EDTA) and centrifuged (266 x g, 4 °C, 4 min) to form a cell pellet. Cell density was determined after resuspension of the cells in fresh medium with a CASY1 model TT cell counter device. Subsequently, the desired amount of cells was washed three times in KHB to remove excess medium.

Cell based assay was carried out in 96 well plates (Greiner, Frickenhausen, Germany) containing 90 µL of the washed cell suspension with 10 µL of the different compound

dilutions to a cell density of about 30,000 cells per well. The plates were incubated for 30 min at 37 °C and 5% CO_2 followed by addition of 20 µl of a 6 µM Hoechst 33342 solution (protected from light) to each well. The prepared plates were then measured with a POLARstar microplate reader (BMG Labtech, Offenburg, Germany) obtaining the fluorescence in constant time intervals (60 s) up to 120 min using an excitation wavelength of 355 nm and an emission wavelength of 460 nm. From the obtained total fluorescence the background induced by the MDCK II cells, potential fluorescence of the compound as well as KHB was subtracted. Average of the fluorescence between 100 and 109 min obtained in the steady state was calculated and plotted against the logarithm of the compound concentration. Dose-response curves were fitted by nonlinear regression using the four-parameter or three-parameter logistic equation whichever was statistically preferred (GraphPad Prism, version 5.0, San Diego, CA, USA).

Calcein AM assay. Selected compounds were investigated for their inhibitory activity toward ABCB1 and ABCC1. Selectivity toward ABCG2 was determined in a calcein AM assay as described in literature.[55,56,57,58,59,60,61,62,63,64,65,66,67,68,69] The ABCB1 overexpressing cell line A2780adr and the ABCC1 overexpressing cell line H69AR were cultured and harvested according to the description in the section "cell culture" above. Washed cells were transferred to the wells of a colorless flat bottom 96 well plate (Greiner, Frickenhausen, Germany) as cell suspension in KHB of a final volume of 90 µL. Then, 10 µL of the corresponding compound was added to each well and the plates incubated at 5 % CO_2 and 37 °C for a period of 30 min. Following, 33 µl of a 1.25 µM calcein AM solution (protected from light) was added quickly to each well and promptly measured in a 37 °C tempered BMG POLARstar microplate reader. Fluorescence was measured over a period of 60 min with constant intervals of 60 s using an excitation wavelength of 485 nm and an emission wavelength of 520 nm to obtain fluorescence-time curves. For this purpose, the slope of the initial linear part of the curves was

calculated to obtain slope-concentration-response curves to each concentration by fitting them with nonlinear regression using the four-parameter or three-parameter logistic equation whichever was statistically preferred.

MTT viability assay. Determination of the intrinsic cytotoxicity of selected compounds was investigated with the MTT cytotoxicity assay as described earlier with slight modifications.[45,46,49,50,51,53,70]

Therefor MDCK II BCRP and parental cells suspended in culture medium were seeded in 96 well tissue culture plates (Sarsted, Newton, USA) at a cell density of approximately 2,000 cells per well using a volume of 180 µL for each well. Plates were incubated under 5% CO_2 and 37 °C for 12 h to allow the cells to attach on the bottom of the wells. Old medium was then removed and quickly replaced with the same volume of fresh medium, followed by addition of 20 µL of different compound dilutions in medium to the wells for a final volume of 200 µL. Prepared plates were incubated for a period of 72 h, storing the plates at 5% CO_2 and 37 °C. Additionally a negative control with solely medium was carried out. After the incubation period of 72 h, 40 µL of MTT reagent (3-(4,5-dimethylthiazol-2-yl)-2,5-diphenyltetrazolium bromide) was added to each well and incubated under the same conditions for an additional hour. Subsequently, the supernatants were removed and 100 µL DMSO added for lysis of the cells and solubilisation of the formed formazan. Measurement of the absorbance was performed with a BMG POLARstar microplate reader at a wavelength of 544 nm and a background correction at 710 nm.

MDR reversal assay. A MDR reversal assay was performed to evaluate a compounds' ability to reverse MDR toward the cytostatic agent and substrate of ABCG2 SN-38, using MDCK II BCRP and parental cells. For this purpose 160 µL of a suspension each containing one of both cell types in culture medium was added to the wells of a clear 96 well tissue culture plate

(Sarsted, Newton, USA) with a cell density of 2,000 cells per well. As described above the plate was incubated and the old medium replaced with the same initial amount of fresh medium. Following, 20 µL of different compound dilutions in culture medium were added to each row together with 20 µL of different dilutions of SN-38 in culture medium added column wise to a final volume of 200 µL. Moreover, a positive control was performed using parental MDCK II cells without modulator. Plates were then incubated for 72 h and prepared as well as measured as described for above in the section "MTT viability assay".

Cells for the MDR reversal assay performed with MX as cytostatic agent were prepared analogously to the method described above for SN-38. Row-wise 20 µL of different compound dilutions in medium was added to the wells with the freshly replaced culture medium. Additionally, 20 µL of either 5 µM MX in culture medium or solely culture medium was added alternating to the rows to a final volume of 200 µL. Moreover, complete cell death was induced by adding 10 % (v/v) DMSO to some of the wells. The plates were then incubated for 72 h at 37 °C and 5% CO_2. Preparation and measurement of the plates was carried out as described above in the section "MTT viability assay".

Protein expression in insect cells and ATPase activity measurements of ABCG2 membranes. For protein expression in High Five ™ insect cells, cells were seeded in culture flasks with Express Five® medium and were incubated at 27 °C. After a few passages when cells were homogenous and healthy, cells were counted and about 20 million cells per flask were seeded for baculovirus infection with Autographa californica multicapsid nuclear polyhedrosis virus (AcMNPV). 72 hours after infection, cells were harvested, centrifuged and afterwards a membrane preparation of the harvested cell pellet was performed.

For this, 1 mL of membrane preparation homogenization buffer (50 mM Tris pH 7.5, 2 mM EGTA pH 7.0, 50 mM Mannitol, 2 mM DTT, 1 mM PMSF, 2 µM pepstatin, 1 µM leupeptin,1 mM benzamidine) was added per 20 million cells. After an incubation period of

30 minutes on ice, cells were disrupted by a dounce homogenizer and the cellular debris was pelleted by centrifugation at 500 × g for 10 min at 4 °C. The resulting pellet was discarded and the supernatant was ultracentrifuged at 300,000 × g for 30 min at 4 °C to obtain a pellet of enriched plasma membranes. Finally membranes were resuspended in 100 µl resuspension buffer (50 mM Tris pH 7.5, 1 mM EGTA at pH 7.0, 10% (v/v) glycerol, 0.3 M mannitol, 1 mM DTT, 1 mM PMSF, 2 µM pepstatin, 1 µM leupeptin, 1 mM benzamidine) per flask and stored at −80 °C until use. [61] ATPase activity measurements of selected compounds was performed by a colorimetric ascorbic acid ammonia molybdate reaction.[71] Vanadate-sensitive basal ATPase activity was compared to vanadate-sensitive drug-stimulated or inhibited activity. Compound **59** was used as standard for ATPase inhibition, quercetin was used as positive control with high stimulation of ABCG2 transport activity. Investigated compounds were dissolved in DMSO, final concentration of DMSO was 1%, which showed no observable effect on basal ATPase activity. All measurements were repeated at least three times.

Concentration-response curves were fitted by nonlinear regression using the three-parameter logistic equation with a fixed Hill slope of one (GraphPad Prism, version 5.0, San Diego, CA, USA).

Inhibition kinetics. To clarify the type of interaction between inhibitor, the substrate Hoechst 33342 and ABCG2, an enzyme kinetic study was carried out. Thus, different compounds were selected and various concentrations of the corresponding compound as well as of Hoechst 33342 (0.4 – 2.4 µM) applied. The remainder of the experimental parameters were chosen as described in the section "Hoechst 33342 accumulation assay". Additionally, the response in the absence of compound was set as control. The obtained values were then used in the Lineweaver-Burk linearization technique as well as the direct linear Cornish-Bowden plot to

confirm the results. Both methods provide information about the underlying interaction-type of the compound with Hoechst 33342.

5D3 antibody binding assay. To estimate the degree of conformational change of ABCG2 in the presence of an inhibitor, the conformational sensitive monoclonal antibody PerCP-Cy^{TM}5.5 Mouse Anti-Human CD338 was employed. The conjugated antibody binds specifically to an epitope of ABCG2, the human CD338 antigen, and emits light at a wavelength of 695 nm upon excitation. Unwanted, non-specific staining was subtracted by using an isotype control. The flow cytometric assay was carried out with mammalian PLB-985 acute myeloid leukemia cell line with an overexpression of ABCG2. Those suspension cells were centrifuged and washed with DPBS containing 0.25% BSA adjusting to a final cell density of 2.5 million cells per mL. 98 µL of the suspension was transferred to a 1.5 mL Eppendorf reaction tube and incubated (37 °C, 5 min, shaking at 500 rpm) with 1 µL of a solution containing DMSO and corresponding compound at the desired concentration. After a 5 minutes preincubation period, 1 µL of the antibody was added and incubation continued for further 30 min. Subsequently, the sample was centrifuged and the liquids removed. The formed cell-pellet was then re-suspended in 1 mL DPBS and immediately measured with a FACSCalibur flow cytometer. For the excitation, a blue laser with an excitation wavelength of 488 nM was used and the fluorescence detected in the FL3 channel. As a comparison, a sample with the same amount of DMSO in the absence of compound was measured as described above. After subtraction of the fluorescence of the isotype control from the fluorescence with the antibody, the median of the corrected fluorescence of the sample with only DMSO was subtracted from the corrected fluorescence in the presence of a compound to obtain a "shift".

Molecular docking. The recent cryo-electron microscopy (cyro-EM) structure of the human ABCG2 transporter (PDB ID: 6FFC) with the fumitremorgin C-related inhibitor, MZ29 was downloaded from RCSB Protein Data Bank.[72] The downloaded structure was prepared using the protein structure preparation tools implemented in Molecular Operating Environment (MOE) 2018.01.[73] The hydrogen atoms for the receptor were assigned according to Protonate-3D module implemented in MOE2018.01. The prepared receptor structure of the human ABCG2 was applied for flexible ligand docking using LeadIT from BioSolveIT, GmbH Germany.[74] During the docking simulations, the ligands were fully flexible while the residues of the receptor were treated as rigid. The binding site for the receptor was defined in 20 Å spacing of the amino acid residues centered based on the ligand, MZ29. By FlexX module implemented in LeadIT, docking of compounds was performed.[75] To predict the binding modes of the compounds, selected compounds were docked into the active site of the receptors using FlexX module implemented in LeadIT. Default docking and scoring parameters were applied and top 100 highest scoring docked positions were stored for further analysis. Each receptor-ligand complex having the lowest binding free energy for interactions was examined and 3D putative binding modes were visualized using MOE2018.01 and PyMOL.[73, 76]

Acknowledgements

We also thank BioSolveIT, GmbH Germany for providing the evaluation license for LeadIT.

Abbreviations Used

ABC, ATP-binding cassette; BCRP, breast cancer resistance protein (ABCG2); cyro-EM, cryo-electron microscopy; MDR, multidrug resistance; MOE, Molecular Operating Environment; MX, mitoxantrone;

Associated Content

Supporting Information

Molecular formula strings and the biological data (CSV)

Accession Codes

PDB accession code: 6FFC (**31**, **41**)

Authors will release the atomic coordinates upon article publication.

Corresponding Author

E-mail: mwiese@uni-bonn

References

(1) Fojo, A. T.; Ueda, K.; Slamon, D. J.; Poplack, D. G.; Gottesman, M. M.; Pastan, I. Expression of a Multidrug-resistance Gene in Human Tumors and Tissues. *Proc. Natl. Acad. Sci. U. S. A.* **1987,** *84*, 265-269.

(2) Mao, Q.; Undakat, J. D. Role of the Breast Cancer Resistance Protein (BCRP/ABCG2) in Drug Transport - an Update. *AAPS J.* **2015,** *17*, 65-82.

(3) McDevitt, C. A.; Collins, R.; Kerr, I. D.; Callaghan, R. Purification and Structural Analyses of ABCG2. *Adv. Drug Deliv. Rev.* **2009,** *61*, 57-65.

(4) Miyake, K.; Mickley, L.; Litman, T.; Zhan, Z.; Robey, R.; Cristensen, B.; Brangi, M.; Greenberger, L.; Dean, M.; Fojo, T.; Bates, S. E. Molecular Cloning of cDNAs Which Are Highly Overexpressed in Mitoxantrone resistant Cells: Demonstration of Homology to ABC Transport Genes. *Cancer Res.* **1999***, 59*, 8-13.

(5) Mo, W.; Zhang, J.-T. Human ABCG2: Structure, Function, and its Role in Multidrug Resistance. *Int. J. Biochem. Mol. Biol.* **2012***, 1*, 1-27.

(6) Wilkens, S. Structure and Mechanism of ABC Transporters. *F1000Prime Rep.* **2015***, 7*, 14.

(7) Zhang, J.-T. Use of Arrays to Investigate the Contribution of ATP-binding Cassette Transporters to Drug Resistance in Cancer Chemotherapy and Prediction of Chemosensitivity. *Cell Res.* **2007,** *17*, 311-323.

(8) Juliano, R. L.; Ling, V. A Surface Glycoprotein Modulating Drug Permeability in Chinese Hamster Ovary Cell Mutants. *Biochim. Biophys. Acta* **1976***, 455*, 152–162.

(9) Cole, S. P.; Bhardwaj, G.; Gerlach, J. H.; Mackie, J. E.; Grant, C. E.; Almquist, K. C.; Stewart, A. J.; Kurz, E. U.; Duncan, A. M.; Deeley, R. G. Overexpression of a Transporter Gene in a Multidrug-Resistant Human Lung Cancer Cell Line. *Science* **1992***, 258*, 1650-1654.

(10) Nakagawa, M.; Schneider, E.; Dixon, K. H.; Horton, J.; Kelley, K.; Morrow, C.; Cowan, K. H. Reduced Intracellular Drug Accumulation in the Absence of P-Glycoprotein (mdrl) Overexpression in Mitoxantrone-Resistant Human MCF-7 Breast Cancer Cells. *Cancer Res.* **1992,** *52*, 6175–6181.

(11) Lemos, C.; Jansen. G.; Peters, G. J. Drug Transporters: Recent Advances Concerning BCRP and Tyrosine Kinase Inhibitors. *Br. J. Cancer* **2008,** *98*, 857-862.

(12) Doyle, L.; Ross, D. D. Multidrug Resistance Mediated by the Breast Cancer Resistance Protein BCRP (ABCG2). *Oncogene* **2003***, 22*, 7340–7358.

(13) Doyle, L. A.; Yang, W.; Abruzzo, L. V.; Krogmann, T.; Gao, Y.; Rishi, A. K.; Ross, D. D. A Multidrug Resistance Transporter from Human MCF-7 Breast Cancer Cells. *Proc. Natl. Acad. Sci.* **1998***, 95*, 15665-15670.

(14) Westover, D.; Li, F. New Trends for Overcoming ABCG2/BCRP-Mediated Resistance to Cancer Therapies. *J. Exp. Clin. Cancer Res.* **2015,** *34*, 3-9.

(15) Xu, J.; Liu, Y.; Yang, Y.; Bates, S.; Zhang, J. T. Characterization of Oligomeric Human Half-ABC Transporter ATP-binding Cassette G2. *J. Biol. Chem.* **2004,** *19*, 19781–19789.

(16) Mc Devitt, C. A.; Collins, R. F.; Conway, M.; Modok, S.; Storm, J.; Kerr, I. D.; Ford, R. C.; Callaghan, R. Purification and 3D Structural Analysis of Oligomeric Human Multidrug Transporter ABCG2. *Structure* **2006***, 14*, 1623–1632.

(17) Hardwick, L.; Velamakanni, S.; van Veen, H. The Emerging Pharmacotherapeutic Significance of the Breast Cancer Resistance Protein (ABCG2). *Br. J. Pharmacol.* **2007,** *151*, 163–174.

(18) Sarkadi, B.; Özvegy-Laczka, C.; Nemet, K.; Váradi, A, ABCG2 – a Transporter for all Seasons. *FEBS Lett.* **2004**, *567*, 116-120.

(19) Wong, K.; Briddon, S. J.; Holliday, N. D.; Kerr, I. D. Plasma Membrane Dynamics and Tetrameric Organisation of ABCG2 Transporters in Mammalian Cells Revealed by Single Particle Imaging Techniques. *Biochim. Biophys. Acta* **2016**, 1863, 19-29.

(20) Gottesman, M. M.; Fojo, T.; Bates, S. E. Multidrug Resistance in Cancer: Role of ATP-Dependent Transporters. *Nat. Rev. Cancer* **2002,** *2*, 48–58.

(21) Choi, C. H. ABC Transporters as Multidrug Resistance Mechanisms and the Development of Chemosensitizers for Their Reversal. *Cancer Cell Int.* **2005,** *5*, 30.

(22) Rosenberg, M. F.; Bikadi, Z.; Chan, J.; Liu, X.; Ni, Z.; Cai, X.; Ford, R. C.; Mao, Q. The Human Breast Cancer Resistance Protein (BCRP/ABCG2) Shows Conformational Changes With Mitoxantrone. *Structure* **2010,** *18*, 482-493.

(23) Doyle, L. A.; Yang, W.; Abruzzo, L. V.; Krogmann, T.; Gao, Y.; Rishi, A. K.; Ross, D. D. A Multidrug Resistance Transporter From Human MCF-7 Breast Cancer Cells. *Proc. Natl. Acad. Sci. U. S. A.* **1998,** *95*, 15665-15670.

(24) Ross, D. D.; Yang, W.; Abruzzo, L. V.; Dalton, W. S.; Schneider, E.; Lage, H.; Dietel, M.; Greenberger, L.; Cole, S. P.; Doyle, L. A. Atypical Multidrug Resistance: Breast Cancer Resistance Protein Messenger RNA Expression in Mitoxantrone-Selected Cell Lines. *J. Natl. Cancer Inst.* **1999,** *91*, 429-433.

(25) Yang, C. J.; Horton, J. K.; Cowan, K. H.; Schneider E. Cross-Resistance to Camptothecin Analogues in a Mitoxantrone-Resistant Human Breast Carcinoma Cell Line is Not Due to DNA Topoisomerase I Alterations. *Cancer Res.* **1995,** *55*, 4004-4009.

(26) Stacy, A. E.; Jansson, P. J.; Richardson, D. R. (2013). Molecular Pharmacology of ABCG2 and its Role in Chemoresistance. *Mol. Pharmacol.* **2013,** *84*, 655-669.

(27) Krapf, M. K.; Wiese, M. Synthesis and Biological Evaluation of 4-Anilino-quinazolines and -quinolines as Inhibitors of Breast Cancer Resistance Protein (ABCG2). *J. Med. Chem.* **2016**, *59*, 5449-5461.

(28) Benderra, Z.; Faussat, A. M.; Sayada, L.; Perrot, J. Y.; Tang, R.; Chaoui, D.; Morjani, H.; Marzac, C.; Marie, J. P.; Legrand, O. MRP3, BCRP, and P-glycoprotein Activities are Prognostic Factors in Adult Acute Myeloid Leukemia. *Clin. Cancer Res.* **2005,** *11*, 7764-7772.

(29) Kim, J. H.; Park, J. M.; Roh, Y. J.; Kim, I. W.; Hasan, T.; Choi, M. G. Enhanced Efficacy of Photodynamic Therapy by Inhibiting ABCG2 in Colon Cancers. *BMC Cancer* **2015,** *15*, 504.

(30) Kim, Y. H.; Ishii, G.; Goto, K.; Ota, S.; Kubota, K.; Murata, Y.; Mishima, M.; Saijo, N.; Nishiwaki, Y.; Ochiai, A. Expression of Breast Cancer Resistance Protein is Associated With a Poor Clinical Outcome in Patients With Small-Cell Lung Cancer. *Lung Cancer* **2009***, 65*, 105-111.

(31) Rabindran, S. K.; He, H.; Singh, M.; Brown, E.; Collins, K. I.; Annable, T.; Greenberger, L. M. Reversal of a Novel Multidrug Resistance Mechanism in Human Colon Carcinoma Cells by Fumitremorgin C. *Cancer Res.* **1998***, 58*, 5850-5858.

(32) Allen, J. D.; van Loevezijn, A.; Lakhai, J. M.; van der Valk, M.; van Tellingen, O.; Reid, G.; Schellens, J. H.; Koomen, G. J. Schinkel, A. H. Potent and Specific Inhibition of the Breast Cancer Resistance Protein Multidrug Transporter in Vitro and in Mouse Intestine by a Novel Analogue of Fumitremorgin C. *Mol. Cancer Ther.* **2002***, 1*, 417–425.

(33) Weidner, L. D.; Zoghbi, S. S.; Lu, S.; Shukla, S.; Ambudkar, S. V.; Pike, V. W.; Mulder, J.; Gottesmann, M. M.; Innis, R. B.; Hall, M. D. The Inhibitor Ko143 is Not Specific for ABCG2. *J. Pharmacol. Exp. Ther.* **2015***, 354*, 384-393.

(34) Barron, G. A., Moseley, H., Woods, J. A. Differential Sensitivity in Cell Lines to Photodynamic Therapy in Combination with ABCG2 Inhibition. *J. Photochem. Photobiol.* **2013***, 126*, 87–96.

(35) Ozvegy-Laczka, C.; Hegedus, T.; Várady, G.; Ujhelly, O.; Schuetz, J. D.; Váradi, A.; Kéri, G.; Orfi, L.; Német, K.; Sarkadi, B. High-affinity Interaction of Tyrosine Kinase Inhibitors with the ABCG2 Multidrug Transporter. *Mol. Pharmacol.* **2004,** *65*, 1485-1495.

(36) Houghton, P. J.; Germain, G. S.; Harwood, F. C.; Schuetz, J. D.; Stewart, C. F.; Buchdunger, E.; Traxler, P. Imatinib Mesylate is a Potent Inhibitor of the ABCG2 (BCRP) Transporter and Reverses Resistance to Topotecan and SN-38 in Vitro. *Cancer Res.* **2004***, 64*, 2333-2337.

(37) Szakács, G.; Hall, M. D.; Gottesman, M. M.; Boumendjel, A.; Kachadourian, R.; Day, B. J.; Baubichon-Cortay, H.; Di Pietro, A. Targeting the Achilles Heel of Multidrug-Resistant Cancer by Exploiting the Fitness Cost of Resistance. *Chem. Rev.* **2014***, 114*, 5753-5774.

(38) Tawar, U.; Jain, A. K.; Dwarakanath, B. S.; Chandra, R.; Singh, Y.; Chaudhury, N. K.; Kaitan, D.; Tandon, V. Influence of Phenyl Ring Disubstitution on Benzimidazole and Terbenzimidazole Cytotoxicity: Synthesis and Evaluation as Radioprotectors. *J. Med. Chem.* **2003**, *46*, 3785-3792.

(39) Krapf, M. K.; Gallus, J.; Wiese, M. 4-Anilino-2-pyridylquinazolines and -pyrimidines as Highly Potent and Nontoxic Inhibitors of Breast Cancer Resistance Protein (ABCG2). *J. Med. Chem.* **2017**, *60*, 4474-4495.

(40) Kraege, S.; Stefan, K.; Juvale, K.; Ross, T.; Willmes, T.; Wiese, M. The Combination of Quinazoline and Chalcone Moieties Leads to Novel Potent Heterodimeric

Modulators of Breast Cancer Resistance Protein (BCRP/ABCG2). *Eur. J. Med. Chem.* **2016**, *117*, 212-229.

(41) Litman, T.; Nielsen, D.; Skovsgaard, T.; Zeuthen, T.; Stein, W.-D. ATPase Activity of P-glycoprotein Related to Emergence of Drug Resistance in Ehrlich Ascites Tumor Cell Lines. *Biochim. Biophys. Acta* **1997**, *1361*, 147-158.

(42) Buxbaum, E. Co-operating ATP Sites in the Multiple Drug Resistance Transporter Mdr1. *Eur. J. Biochem.* **1999**, 265, 54-63.

(43) Telbisz, Á.; Hegedüs, C.; Özvegy-Laczka, C.; Goda, K.; Váradym, G.; Takáts, Z.; Szabo, E.; Sorrentino, B. P.; Varadi, A.; Sarkadi, B. Antibody Binding Shift Assay for Rapid Screening of Drug Interactions With the Human ABCG2 Multidrug Transporter. *Eur. J. Pharm. Sci.* **2012***, 45*, 101-109.

(44) Taylor, N. M. I.; Manolaridis, I.; Jackson, S. M.; Kowal, J.; Stahlberg, H.; Locher, K. P. Structure of the Human Multidrug Transporter ABCG2. *Nature* **2017**, *546*, 504-509.

(45) Jackson, S. M.; Manolaridis, I.; Kowal, J.; Zechner, M.; Taylor, N. M. I.; Bause, M.; Bauer, S.; Bartholomaeus, R.; Bernhardt, G.; Koenig, B.; Buschauer, A.; Stahlberg, H.; Altmann, K.-H.; Locher, K. P., Structural Basis of Small-Molecule Inhibition of Human Multidrug Transporter ABCG2. *Nat. Struct. Mol. Biol.* **2018,** *25*, 333-340.

(46) Khunweeraphong, N.; Stockner, T.; Kuchler, K. The Structure of the Human ABC Transporter ABCG2 Reveals a Novel Mechanism for Drug Extrusion. *Scientific Reports*, **2017**, *7*, 13767.

(47) Laszlo, L.; Sarkadi, B.; Hegedus, T., Jump into a New Fold - A Homology Based Model for the ABCG2/BCRP Multidrug Transporter. *PLoS One* **2016,** *11*, e0164426.

(48) Ni, Z.; Bikadi, Z.; Cai, X.; Rosenberg, M. F.; Mao, Q., Transmembrane Helices 1 and 6 of the Human Breast Cancer Resistance Protein (BCRP/ABCG2): Identification of

Polar Residues Important for Drug Transport. *Am. J. Physiol. Cell Physiol.* **2010,** *299*, C1100-11009.

(49) Honjo, Y.; Hrycyna, C. A.; Yan, Q. W.; Medina-Perez, W. Y.; Robey, R. W.; van de Laar, A.; Litman, T.; Dean, M.; Bates, S. E., Acquired Mutations in the MXR/BCRP/ABCP Gene Alter Substrate Specificity in MXR/BCRP/ABCP-Overexpressing Cells. *Cancer Res.* **2001,** *61*, 6635-6639.

(50) Ozvegy, C.; Varadi, A.; Sarkadi, B., Characterization of Drug Transport, ATP Hydrolysis, and Nucleotide Trapping by the Human ABCG2 Multidrug Transporter. Modulation of Substrate Specificity by a Point Mutation. *J. Biol. Chem.* **2002,** *277*, 47980-47990.

(51) Volk, E. L.; Farley, K. M.; Wu, Y.; Li, F.; Robey, R. W.; Schneider, E., Overexpression of Wild-Type Breast Cancer Resistance Protein Mediates Methotrexate Resistance. *Cancer Res.* **2002,** *62*, 5035-5040.

(52) Tamura, A.; Watanabe, M.; Saito, H.; Nakagawa, H.; Kamachi, T.; Okura, I.; Ishikawa, T., Functional Validation of the Genetic Polymorphisms of Human ATP-binding Cassette (ABC) Transporter ABCG2: Identification of Alleles that are Defective in Porphyrin Transport. *Mol. Pharmacol.* **2006,** *70*, 287-296.

(53) Porohit, V.; Basu, A. Mutagenicity of nitroaromatic compounds. *Chem. Res. Toxicol.* **2000**, *13*, 673–692.

(54) Pick, A.; Müller, H.; Wiese, M. Structure-activity Relationships of New Inhibitors of Breast Cancer Resistance Protein (ABCG2). *Bioorg. Med. Chem.* **2008**, *16*, 8224–8236.

(55) Pick, A.; Wiese, M. Tyrosine Kinase Inhibitors Influence ABCG2 Expression in EGFR-Positive MDCK BCRP Cells Via the PI3K/Akt Signaling Pathway. *ChemMedChem,* **2012,** *7*, 650-662.

(56) Juvale, K.; Wiese, M. 4-Substituted-2-phenylquinazolines as Inhibitors of BCRP. *Bioorg. Med. Chem. Lett.* **2012,** *22*, 6766−6769.

(57) Pick, A.; Klinkhammer, W.; Wiese, M. Specific Inhibitors of the Breast Cancer Resistance Protein (BCRP). *ChemMedChem.* **2010**, *5*, 1498–1505.

(58) Marighetti, F.; Steggemann, K.; Hanl, M.; Wiese, M. Synthesis and Quantitative Structure-Activity Relationships of Selective BCRP Inhibitors. *ChemMedChem* **2013**, *8*, 125–135.

(59) Marighetti, F.; Steggemann, K.; Karbaum, M.; Wiese, M. Scaffold Identification of a New Class of Potent and Selective BCRP-inhibitors. *ChemMedChem* **2015**, *10*, 742–751.

(60) Pick, A.; Müller, H.; Mayer, R.; Haenisch, B.; Pajeva, I. K.; Weigt, M.; Bönisch, H.; Müller, C. E.; Wiese, M. Structure-Activity Relationships of Flavonoids as Inhibitors of Breast Cancer Resistance Protein (BCRP). *Bioorg. Med. Chem.* **2011**, *19*, 2090−2102.

(61) Müller, H.; Klinkhammer, W.; Globisch, C.; Kassack, M. U.; Pajeva, I. K.; Wiese, M. New Functional Assay of P-glycoprotein Activity Using Hoechst 33342. *Bioorg. Med. Chem.* **2007**, *15*, 7470−7479.

(62) Juvale, K.; Pape, V. F.; Wiese, M. Investigation of Chalcones and Benzochalcones as Inhibitors of Breast Cancer Resistance Protein. *Bioorg. Med. Chem.* **2012**, *20*, 346-355.

(63) Singh, M. S.; Juvale, K.; Wiese, M.; Lamprecht, A. Evaluation of Dual P-gp-BCRP Inhibitors as Nanoparticle Formulation. *Eur. J. Pharm. Sci.* **2015**, *77*, 1-8.

(64) Juvale, K.; Stefan, K.; Wiese, M. Synthesis and Biological Evaluation of Flavones and Benzoflavones as Inhibitors of BCRP/ABCG2. *Eur. J. Med. Chem.* **2013**, *67*, 115−126.

(65) Müller, H.; Pajeva, I. K.; Globisch, C.; Wiese, M. Functional Assay and Structure-Activity Relationships of New Third-Generation P-glycoprotein Inhibitors. *Bioorg. Med. Chem.* **2008**, *16*, 2456−2470.

(66) Köhler, S. C.; Wiese, M. HM30181 Derivatives as Novel Potent and Selective Inhibitors of the Breast Cancer Resistance Protein (BCRP/ABCG2). *J. Med. Chem.* **2015**, *58*, 3910−3921.

(67) Leyers, S., Häcker, H.-G.; Wiendlocha, J.; Gütschow, M.; Wiese, M. A 4-aminobenzoic Acid Derivative as Novel Lead For Selective Inhibitors of Multidrug Resistance-Associated Proteins, *Bioorg. Med. Chem*. *Lett.* **2008**, *18*, 4761-4763.

(68) Klinkhammer, W.; Müller, H.; Globisch, C.; Pajeva, I. K.; Wiese, M. Synthesis and Biological Evaluation of a Small Molecule Library of 3rd Generation Multidrug Resistance Modulators, *Bioorg. Med. Chem.* **2009**, *17*, 2524-2535.

(69) Häcker, H.-G.; Leyers, S.; Wiendlocha, J.; Gütschow, M.; Wiese, M. Aromatic 2-(Thio)ureidocarboxylic Acids As a New Family of Modulators of Multidrug Resistance-Associated Protein 1: Synthesis, Biological Evaluation, and Structure-Activity Relationships. *J. Med. Chem.* **2009**, *52*, 4586-4595.

(70) Gallus, J.; Juvale, K.; Wiese, M. Characterization of 3-Methoxy Flavones for Their Interaction With ABCG2 as Suggested by ATPase Activity. *Biochim. Biophys. Acta* **2014**, *1838*, 2929-2938.

(71) Sarkadi, B.; Price, E. M.; Boucher R. C.; Germann U. A.; Scarborough G. A. Expression of the Human Multidrug Resistance cDNA in Insect Cells Generates a High Activity Drug-Stimulated Membrane ATPase. *J. Biol. Chem.* **1992**, *267*, 4854-4858.

(72) Jackson, S. M.; Manolaridis, I.; Kowal, J.; Zechner, M.; Taylor, N. M. I.; Bause, M.;

Bauer, S.; Bartholomaeus, R.; Bernhardt, G.; Koenig, B.; Buschauer, A.; Stahlberg, H.; Altmann, K.-H.; Locher, K. P. Structural Basis of Small-Molecule Inhibition of Human Multidrug Transporter ABCG2. *Nat. Struct. Mol. Biol.* **2018,** *25*, 333-340.

(73) *Molecular Operating Environment (MOE), 2013.08; Chemical Computing Group ULC, 1010 Sherbooke St. West, Suite #910, Montreal, QC, Canada, H3A 2R7*, **2017**.

(74) *LeadIT version 2.3.2; BioSolveIT GmbH, Sankt Augustin, Germany.*, **2017**.

(75) Rarey, M.; Kramer, B.; Lengauer, T.; Klebe, G. A Fast Flexible Docking Method Using an Incremental Construction Algorithm. *J. Mol. Biol.* **1996,** *261*, 470-489.

(76) *The PyMOL Molecular Graphics System, Version 1.8. Schrodinger, LLC*, **2015**.

Scheme 1. General Synthesis Route for Compounds **1-51**.[a]

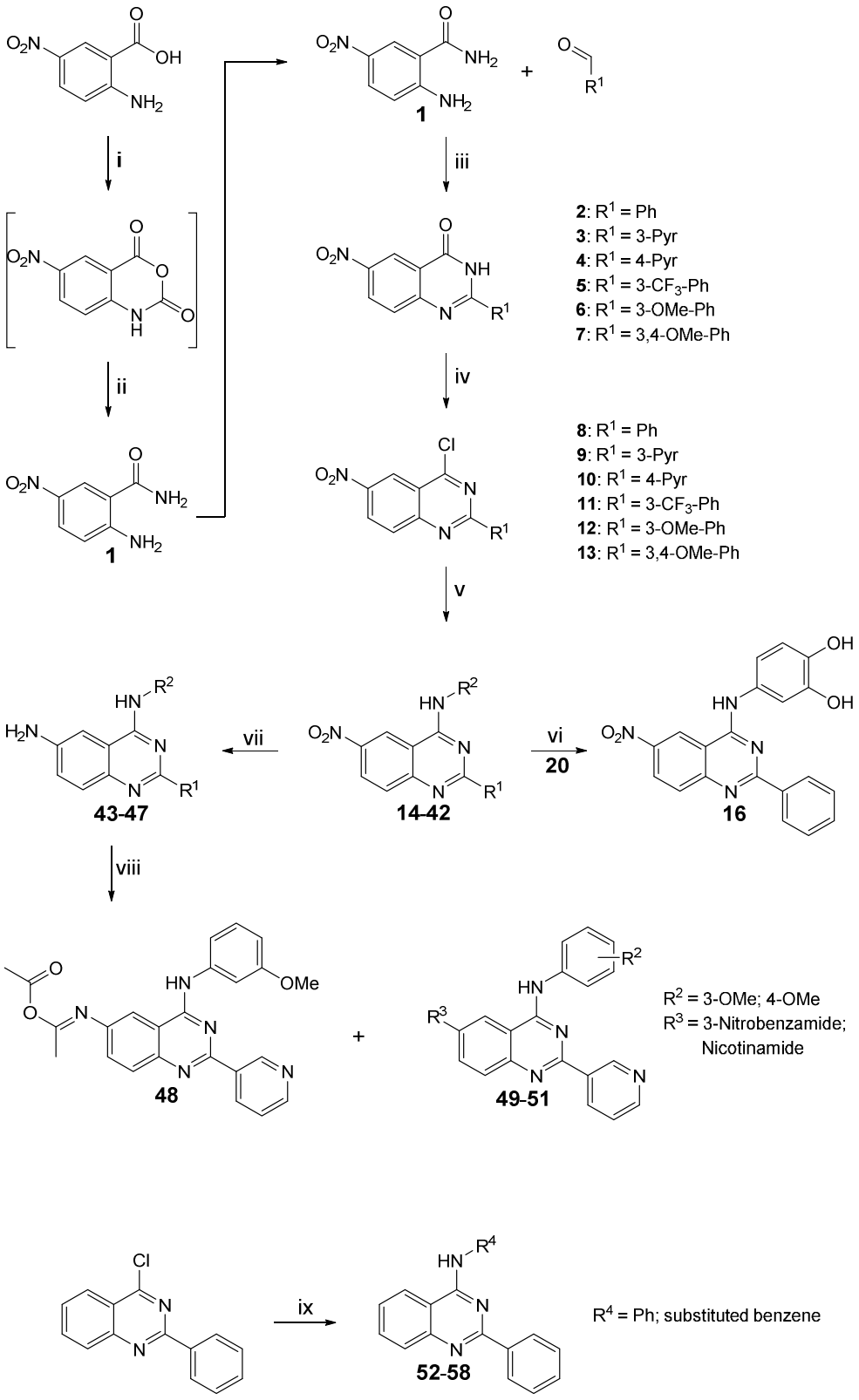

[a] Reagents and conditions: (i) Triphosgene, THF, reflux, 3h. (ii) NH_3, 50 °C, 30 min. (iii) I_2, K_2CO_3, DMF, 90-110 °C, 8-12 h (iv) $POCl_3$, reflux, 4-12 h. (v) *i*-PrOH, substituted aniline, 100 watt microwave irradiation, 110 °C, 20-40 min. (vi) BBr_3, DCM, -60°C → RT, 12 h. (vii) THF, 4 bar H_2, Pd/C, RT, 24 h. (viii) RCOCl, THF, 0 °C → RT, 6-12 h. (ix) *i*-PrOH, substituted aniline, 100 watt microwave irradiation, 110 °C, 30 min.

Table 1. Inhibitory Activities Derived from the Hoechst 33342 Accumulations Assay Toward ABCG2 Overexpressing MDCK II Cell Line. The Scaffold with Substitution Pattern is Illustrated Below.

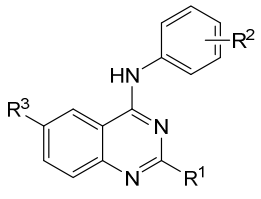

Compd.	R^1	R^2	R^3	Hoechst 33342 IC_{50} ± SD [nM][a]
14	Ph	H	NO_2	106 ± 15
15	Ph	3-OH	NO_2	65.3 ± 9.7
16	Ph	3,4-OH	NO_2	119 ± 17
17	Ph	3-OMe	NO_2	33.1 ± 5.6
18	Ph	3,4-OMe	NO_2	37.0 ± 5
19	Ph	3-CN	NO_2	48.2 ± 7.7
20	Ph	4-CN	NO_2	48.1 ± 9.2
21	Ph	3-F	NO_2	51.5 ± 9.8
22	Ph	3-CF_3	NO_2	49.1 ± 5.8
23	Ph	3-NO_2-4-OH	NO_2	37.4 ± 5.0
24	Ph	3-$NHCOCH_3$	NO_2	78.7 ± 13.5
25	Ph	3-CO_2H	NO_2	904 ± 17
26	3-Pyr	3-OMe	NO_2	47.0 ± 4.0
27	3-Pyr	4-OMe	NO_2	57.7 ± 7.0
28	4-Pyr	4-OMe	NO_2	75.5 ± 14.4
29	4-Pyr	3-CN	NO_2	63.8 ± 13.2
30	3-CF_3-Ph	H	NO_2	59.6 ± 8.00
31	3-CF_3-Ph	3-OH	NO_2	27.6 ± 2.4
32	3-CF_3-Ph	3-OMe	NO_2	59.0 ± 5.9
33	3-CF_3-Ph	3,4-OMe	NO_2	30.2 ± 4.3
34	3-CF_3-Ph	3-SMe	NO_2	101 ± 16
35	3-CF_3-Ph	3-F	NO_2	44.8 ± 6.2
36	3-CF_3-Ph	3-NO_2	NO_2	66.3 ± 13.3
37	3-CF_3-Ph	4-NO_2	NO_2	61.4 ± 5.7
38	3-CF_3-Ph	3-NO_2-4-OH	NO_2	33.0 ± 4.7
39	3-CF_3-Ph	3-$NHCOCH_3$	NO_2	44.8 ± 4.4
40	3-OMe-Ph	4-CN	NO_2	27.8 ± 3.8
41	3-OMe-Ph	3-F	NO_2	23.4 ± 3.4
42	3,4-OMe-Ph	3-CF_3	NO_2	57.2 ± 7.9
43	3-Pyr	3-OMe	NH_2	369 ± 54
44	3-Pyr	4-OMe	NH_2	646 ± 69
45	3-CF_3-Ph	H	NH_2	726 ± 49
46	3-CF_3-Ph	3-OH	NH_2	799 ± 159

47	3-CF_3-Ph	3-OMe	NH_2	835 ± 113
48	3-Pyr	3-OMe	*N*-1-Iminoethyl acetate	5310 ± 240
49	3-Pyr	3-OMe	*N*-3-Nitrobenzamide	1150 ± 190
50	3-Pyr	4-OMe	*N*-3-Nitrobenzamide	1620 ± 70
51	3-Pyr	3-OMe	*N*-Nicotinamide	1040 ± 80
52[b]	Ph	H	H	882 ± 157
53[b]	Ph	3,4-OMe	H	152 ± 19
54[c]	Ph	4-CN	H	69.9 ± 10
55[c]	Ph	3-F	H	355 ± 53
56[c]	Ph	3-NO_2-4-OH	H	80.0 ± 9.1
57[c]	Ph	3-$NHCOCH_3$	H	278 ± 33
58[c]	Ph	3-CO_2H	H	6380 ± 1390
59[d]				227 ± 14

[a] *IC_{50} values are means of three independent experiments.*
[b] *Compounds synthesized in earlier study.*[46]
[c] *IC_{50} values taken from our previous study.*[27]
[d] *Used as reference in the assay.*

Table 2. Intrinsic Toxicity of Selected Compounds in ABCG2 Overexpressing MDCK II BCRP and Parental Cells.

Compd	R^1	R^2	R^3	GI_{50} [μM][a] BCRP	GI_{50} [μM][a] Parental	Therapeutic ratio (GI_{50}/IC_{50})[d]
14	Ph	H	NO_2	18.3	36.1	173
17	Ph	3-OMe	NO_2	5.50	6.92	166
18	Ph	3,4-OMe	NO_2	8.13	8.51	220
23	Ph	3-NO_2-4-OH	NO_2	13.2	9.75	353
28	4-Pyr	4-OMe	NO_2	84.5	125	1119
29	4-Pyr	3-CN	NO_2	77.3	104	1212
31	3-CF_3-Ph	3-OH	NO_2	3.39	3.02	123
33	3-CF_3-Ph	3,4-OMe	NO_2	3.63	3.16	120
38	3-CF_3-Ph	3-NO_2-4-OH	NO_2	27.4	24.1	830
40	3-OMe-Ph	4-CN	NO_2	11.0	9.12	395
41	3-OMe-Ph	3-F	NO_2	4.38	11.2	187
44	3-Pyr	4-OMe	NH_2	19.1	27.5	29.6
52[b]	Ph	H	H	26.6	26.0	30.1
53[b]	Ph	3,4-OMe	H	22.5	17.0	148
56[c]	Ph	3-NO_2-4-OH	H	52.4	152	655
59				12.6	12.5	55.5

[a] Concentration accomplishing 50 % of cell survival with MDCK II BCRP and parental cells, respectively. The data was obtained from at least two independent experiments as mean values.
[b] Compounds synthesized in earlier study.[46]
[c] GI_{50} value taken from our previous study.[27]
[d] Therapeutic ratio was calculated from the quotient of the GI_{50} [μM] obtained with BCRP expressing cells and the IC_{50} [μM] obtained from the Hoechst 33342 assay.

Table 3. EC_{50} values of selected compounds in the ATPase activity assay. All values are relative vanadate-sensitive ATPase activities in relation to the basal activity, which is set to 100%. Compounds **14**, **17**, **21**, **31**, **32**, **37**, **41** and **44** had no observable effect on ATPase activity.

Activating Compounds	**EC_{50} [nM][b]**	**V_{max} [% of control]**
18	63	136
19	326	135
20	29	135
26	690	168
28	112	134
30	48	152
40	10	143
47	1230	168
Quercetin [a)]	278	177

Compounds with biphasic behavior	**Concentration of maximal activity [nM]**	**V_{max} [% of control]**
22	1000	138
27	1000	115
33	35	131
43	250	122

[a]: *Compound tested in earlier study* [39]
[b]: *Results were obtained by at least two independent experiments.*

Table 4. Compounds interaction type with Hoechst 33342 derived from the Lineweaver-Burk Double Reciprocal Plot.

Comp.	R^1	R^2	R^3	Intersection[a]	Kinetic type of interaction with Hoechst 33342
17	Ph	3-OMe	NO_2	2. Quadrant	Non-competitive mixed-type
27	3-Pyr	4-OMe	NO_2	2. Quadrant	Non-competitive mixed-type
31	3-CF_3-Ph	3-OH	NO_2	Y-axis	Competitive
40	3-OMe-Ph	4-CN	NO_2	2. Quadrant	Non-competitive mixed-type
41	3-OMe-Ph	3-F	NO_2	3. Quadrant	Non-competitive mixed-type
43	3-Pyr	3-OMe	NH_2	2. Quadrant	Non-competitive mixed-type
44	3-Pyr	4-OMe	NH_2	3. Quadrant	Non-competitive mixed-type
47	3-CF_3-Ph	3-OMe	NH_2	2. Quadrant	Non-competitive mixed-type
59				2. Quadrant	Non-competitive mixed-type

[a]: Intersection point of the family of lines resulting from the Lineweaver-Burk method (Figure 8).

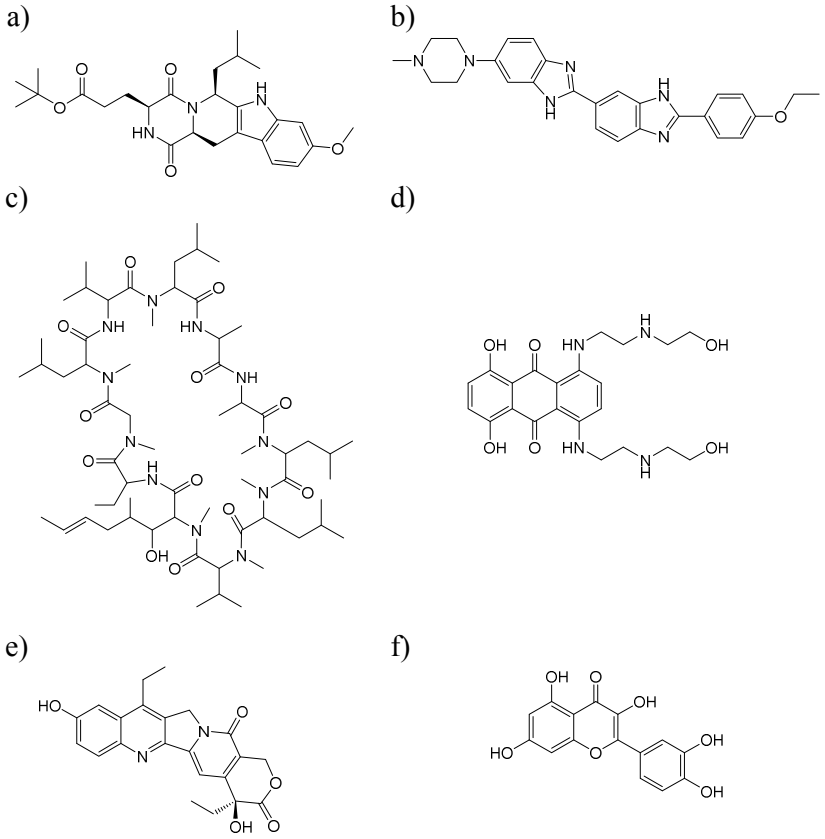

Figure 1. Molecular structures of the reference compounds **59** (Ko143, a), Hoechst 33342 (b), cyclosporine A (CsA, c), mitoxantrone (MX, d), the active metabolite of irinotecan (SN-38, e) and quercetine (f).

a)

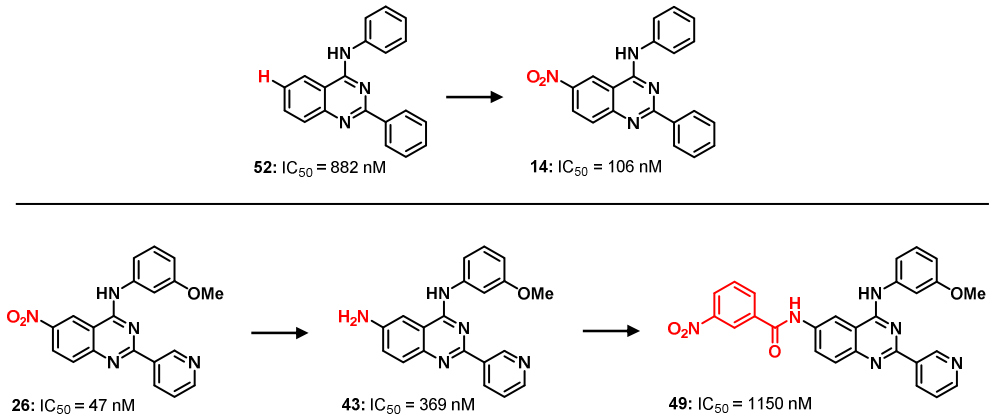

b)

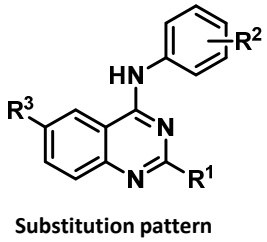

Compd.	R^1	R^2	R^3
17	Ph	3-OMe	NO_2
18	Ph	3,4-OMe	NO_2
31	3-CF_3-Ph	3-OH	NO_2
33	3-CF_3-Ph	3,4-OMe	NO_2
40	3-OMe-Ph	4-CN	NO_2
41	3-OMe-Ph	3-F	NO_2
24	Ph	3-$NHCOCH_3$	NO_2
14	Ph	H	NO_2
34	3-CF_3-Ph	3-SMe	NO_2
43	3-Pyr	3-OMe	NH_2
44	3-Pyr	4-OMe	NH_2
45	3-CF_3-Ph	H	NH_2
46	3-CF_3-Ph	3-OH	NH_2
47	3-CF_3-Ph	3-OMe	NH_2
25	Ph	3-CO_2H	NO_2
6-N-substituted compounds (**48-51**)			

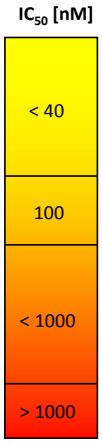

Figure 2. SAR of some compounds illustrating structural features impacting the inhibitory potency of a compound. Highest potencies were achieved by 6-nitro derivatives, notably by those containing methoxy or hydroxy functions (a). Regarding substitution at position 6, lower inhibitory potencies resulted from 6-amino (**43-47**) and 6-*N*-functionalized (**48-51**) derivatives compared to nitro (b).

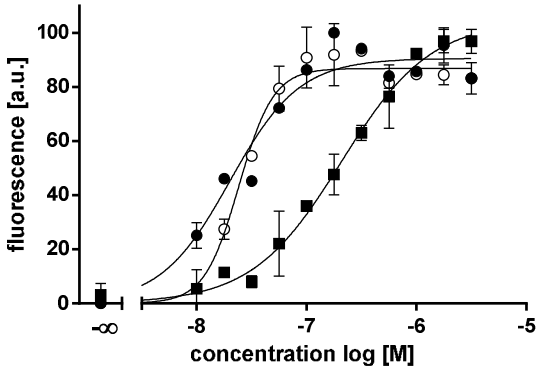

Figure 3. Compounds **40** (open circle, IC_{50} = 27.8 nM) and **41** (closed circle, IC_{50} = 23.4 nM) in a Hoechst 33342 accumulation assay with compound **59** (closed square, IC_{50} = 227 nM) as reference, using the ABCG2 overexpressing MDCK II BCRP cell line.

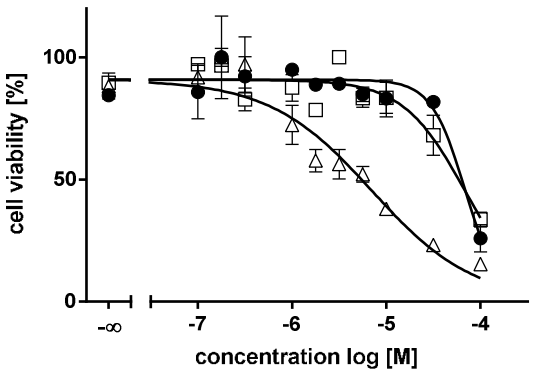

Figure 4. Representative examples of MTT viability assays of compounds **28** (□), **29** (●), and **41** (Δ) using the ABCG2 overexpressing MDCK II BCRP cell line. The GI_{50} values were determined as 84.5 µM (□), 77.3 µM (○) and 9.46 µM (Δ), respectively.

a)

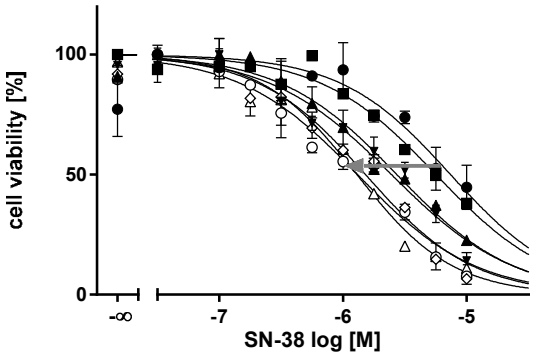
cell viability [%]
100
50
0
-∞
-7
-6
-5
SN-38 log [M]

b)

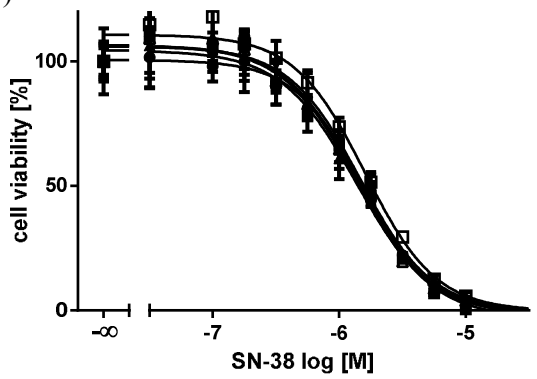
cell viability [%]
100
50
0
-∞
-7
-6
-5
SN-38 log [M]

c)

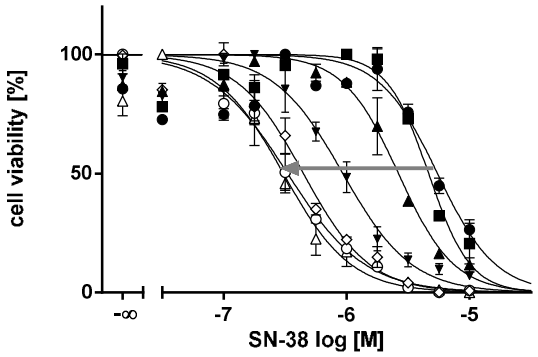
cell viability [%]
100
50
0
-∞
-7
-6
-5
SN-38 log [M]

d)

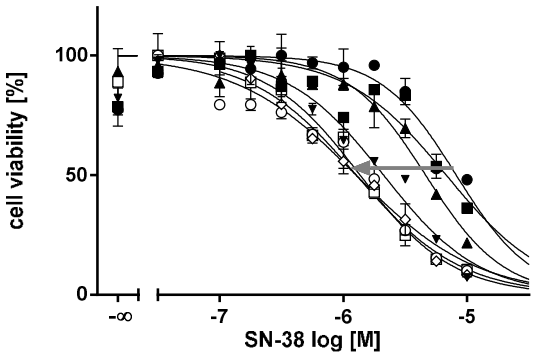
cell viability [%]
100
50
0
-∞
-7
-6
-5
SN-38 log [M]

Figure 5. MDR reversal assay to determine the ability of compound **23**, **28**, and **41** to reverse the MDR against the cytostatic drug SN-38, using the ABCG2 overexpressing cell line (a, c, d). The following concentrations were used: control (closed circle), 0.01 μM (closed square), 0.03 μM (closed triangle), 0.1 μM (closed down triangle), 1 μM (open triangle), 5 μM (open square), parental cell line (open circle).The grey arrow indicates the increasing sensitization of the ABCG2 overexpressing cells with higher compound concentrations. At a compound concentration of 1 μM, full reversal is achieved, indicated by a similar pGI_{50} as the parental cells. Exemplarily is shown for compound **23** that there is no effect on the parental MDCK II cells (b).

a)

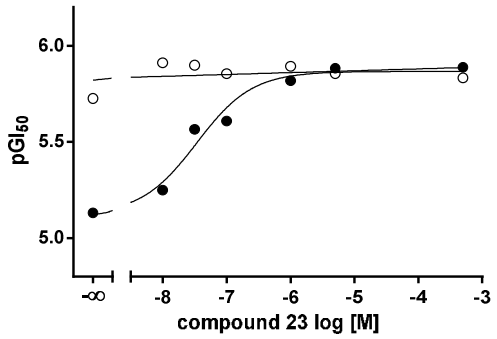

b)

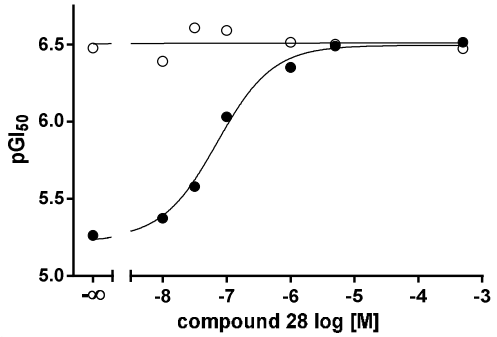

c)

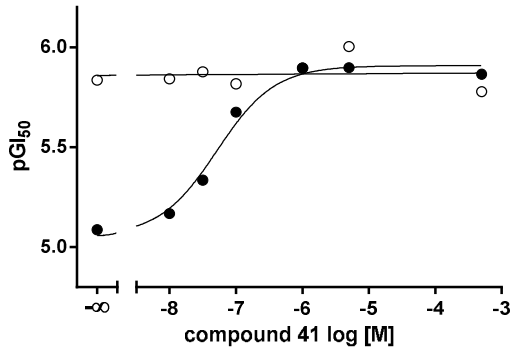

Figure 6. Nonlinear regression of the pGI_{50} values determined in the MDR reversal assay (Figure 5 a, c, d) against the corresponding concentration of compounds **23**, **28** and **41**. EC_{50} is the concentration that reduces resistance of the ABCG2 overexpressing cells to 50%. The following EC_{50} values were calculated: 34.0 nM (**23**), 71.2 nM (**28**) and 51.5 nM (**41**).

The pGI_{50} values of the parental cells determined in an analogous assay are depicted by open circles.

a)

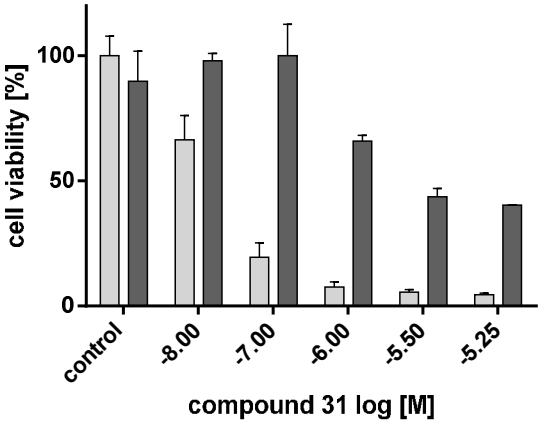

b)

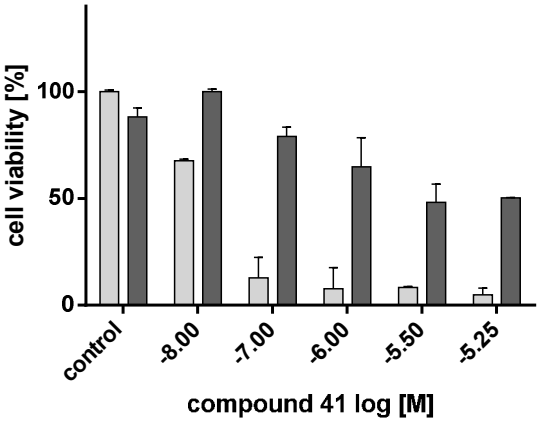

Figure 7. MDR reversal assay of compounds **31** (a, EC_{50}: 21.8 nM) and **41** (b, EC_{50}: 19.5 nM), demonstrating their ability to reverse MDR toward the cytostatic MX, using the ABCG2 overexpressing cell line MDCK II. The bars represent the cell viability at a given modulator concentration in the presence (light grey) and absence (dark grey) of 0.5 μM MX. The standard deviation is expressed by error bars.

a)

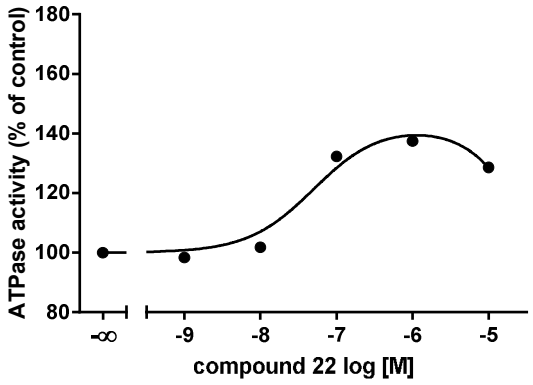

b)

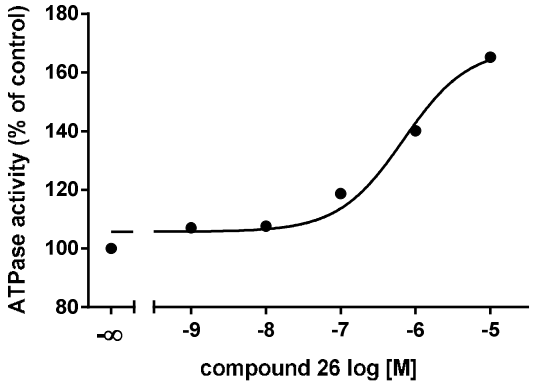

c)

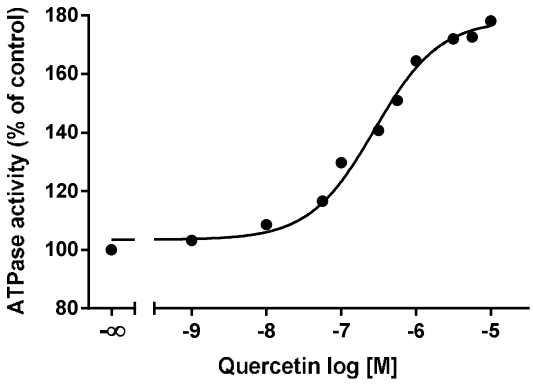

Figure 8. Concentration-response curves for compounds **22** (a), **26** (b) and **Quercetin** (c) in the ATPase activity assay. All values are vanadate-sensitive ATPase activities in relation to the basal activity, which is set to 100%.

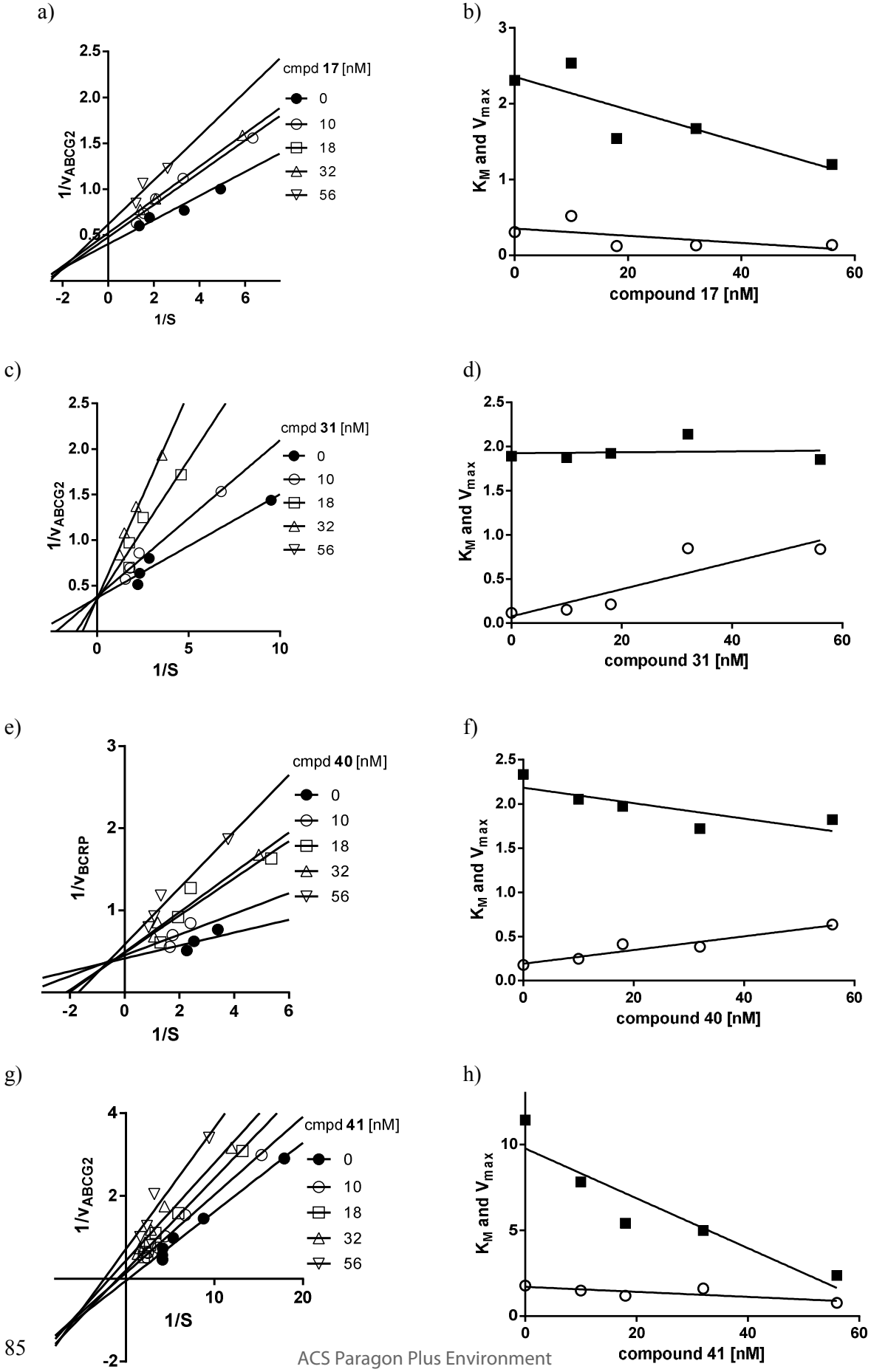
a)
b)
c)
d)
e)
f)
g)
h)
cmpd 17 [nM]
cmpd 31 [nM]
cmpd 40 [nM]
cmpd 41 [nM]
0
10
18
32
56
1/V_ABCG2
1/V_BCRP
1/S
K_M and V_max
compound 17 [nM]
compound 31 [nM]
compound 40 [nM]
compound 41 [nM]

Figure 9. Lineweaver–Burk plot for compounds **17** (a), **31** (c), **40** (e) and **41** (g) at various concentrations together with the ABCG2 substrate Hoechst 33342. Plot of the Michaelis-Menten constant K_M (open circle) and the maximum velocity V_{max} (closed square) derived from the analysis according to Cornish-Bowden against the corresponding compound concentration (**17** b), **31** d), **40** f), **41**, h)).

a) b)

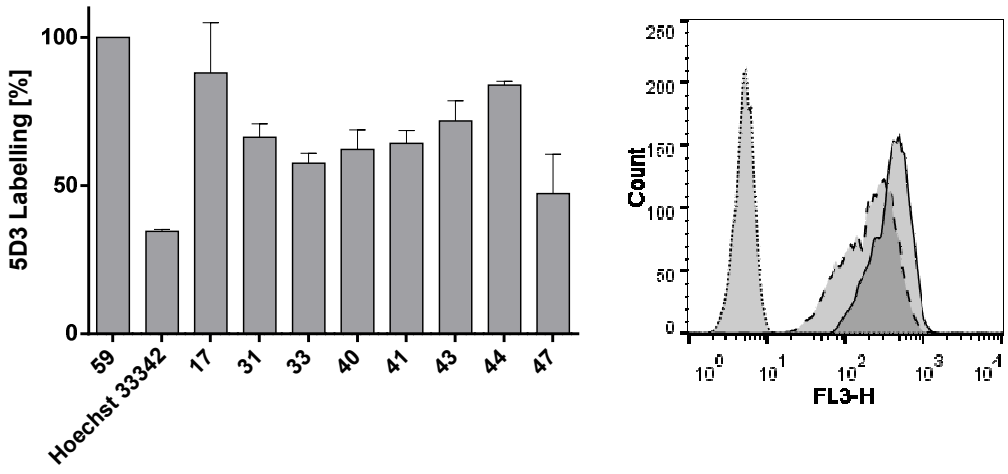

Figure 10. (a) 5D3 immunoreactivity modulation of ABCG2 by various compounds at a concentration of 10 μM. Fluorescence detected by the 5D3-labeling of ABCG2 in the presence of 10 μM compound **59** was set to 100% and the fluorescence measured in the absence of any compound taken as 0%. Values are means of at least three independent experiments and the SD is given as error bar. (b) Histogram of the obtained fluorescence at the FL3-H detector (X-axis) and the cell-count according to the corresponding fluorescence. Depicted is the fluorescence of the isotype-control (dotted curve) as well as of 5D3 antibody in the absence of a compound **59** (dashed curve) and in the presence of compound **59** (continuous curve).

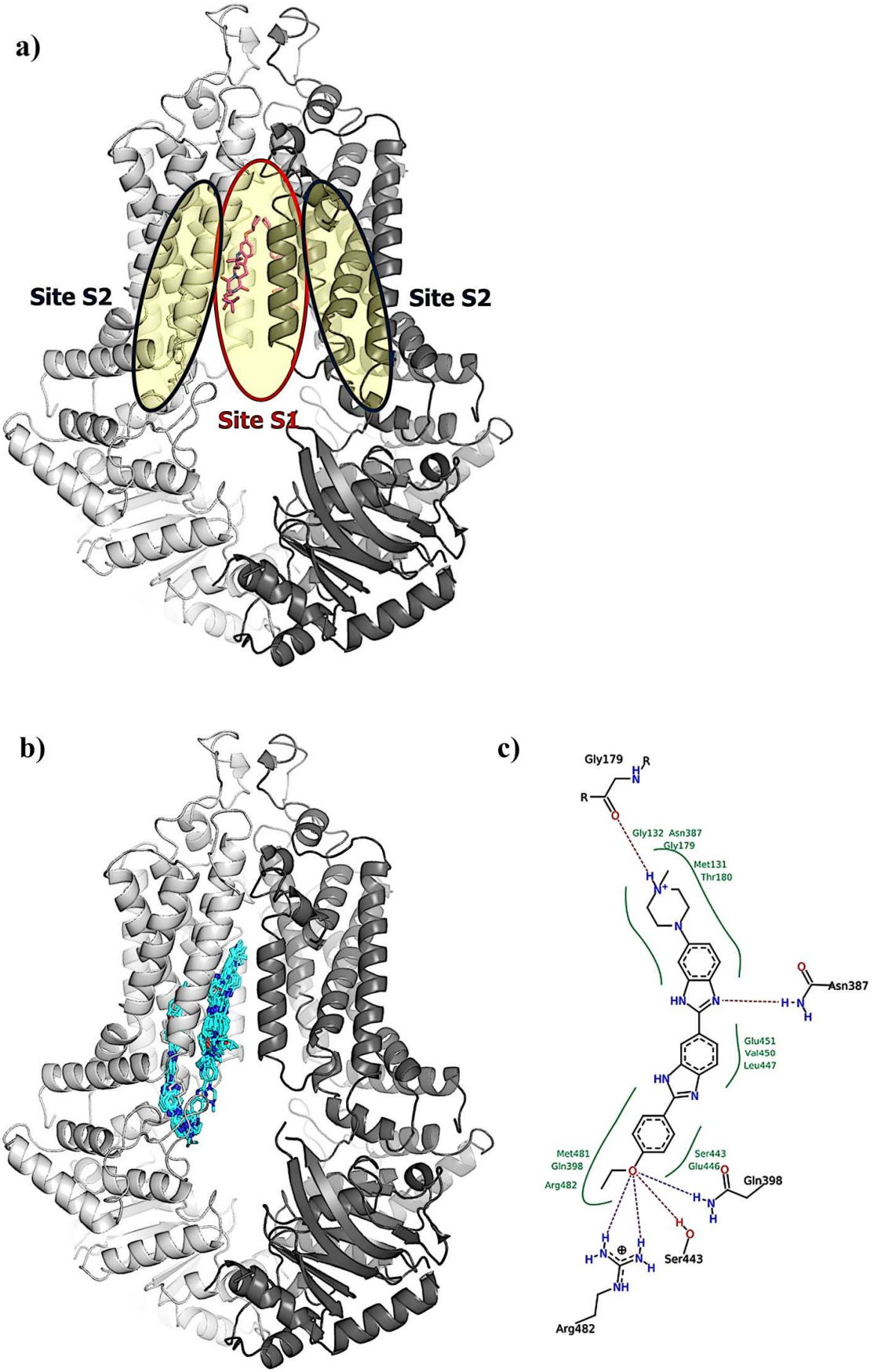
a)
Site S2
Site S2
Site S1
b)
c)
Gly179
Gly132
Asn387
Gly179
Met131
Thr180
Asn387
Glu451
Val450
Leu447
Met481
Gln398
Arg482
Ser443
Glu446
Gln398
Ser443
Arg482

Figure 11. Binding poses of MZ29 and Hoechst 33342. (a) The binding pose of the inhibitor MZ29 (purple) observed in the cryo-EM structure of the human ABCG2 receptor (PDB ID: 6FFC). The putative binding sites of the human ABCG2 receptor are schematically indicated as S1 and S2 (b) Docked poses of the substrate Hoechst 33342 in the binding pockets of the human ABCG2 receptor and (c) 2D interaction diagram. The human ABCG2 receptor (chain A, gray and chain B dark gray) is displayed in cartoon representation. Both MZ29 and Hoechst 33342 are shown as stick models. Oxygen atoms are colored in red and nitrogen atoms in blue.

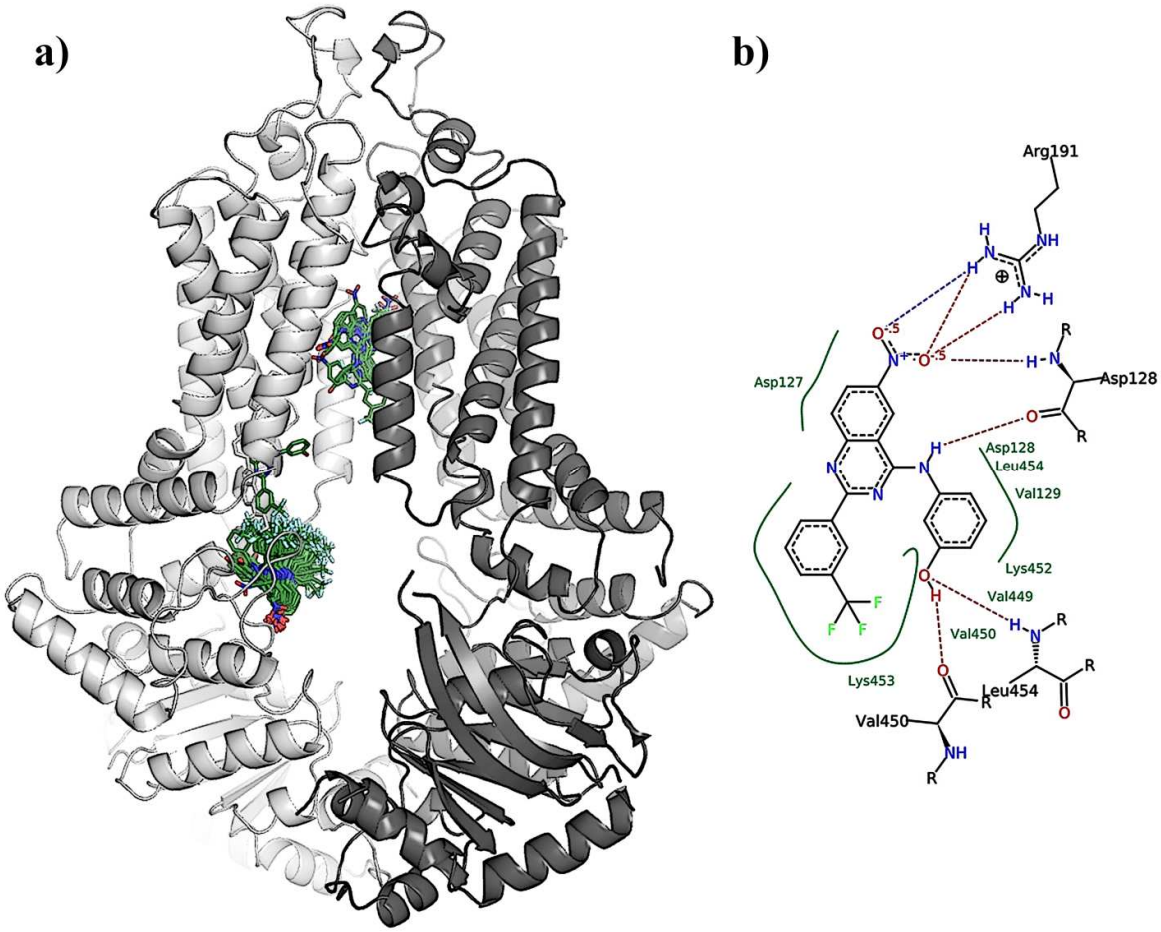
a)
b)
Arg191
Asp127
Asp128
Asp128
Leu454
Val129
Lys452
Val449
Val450
Lys453
Leu454
Val450

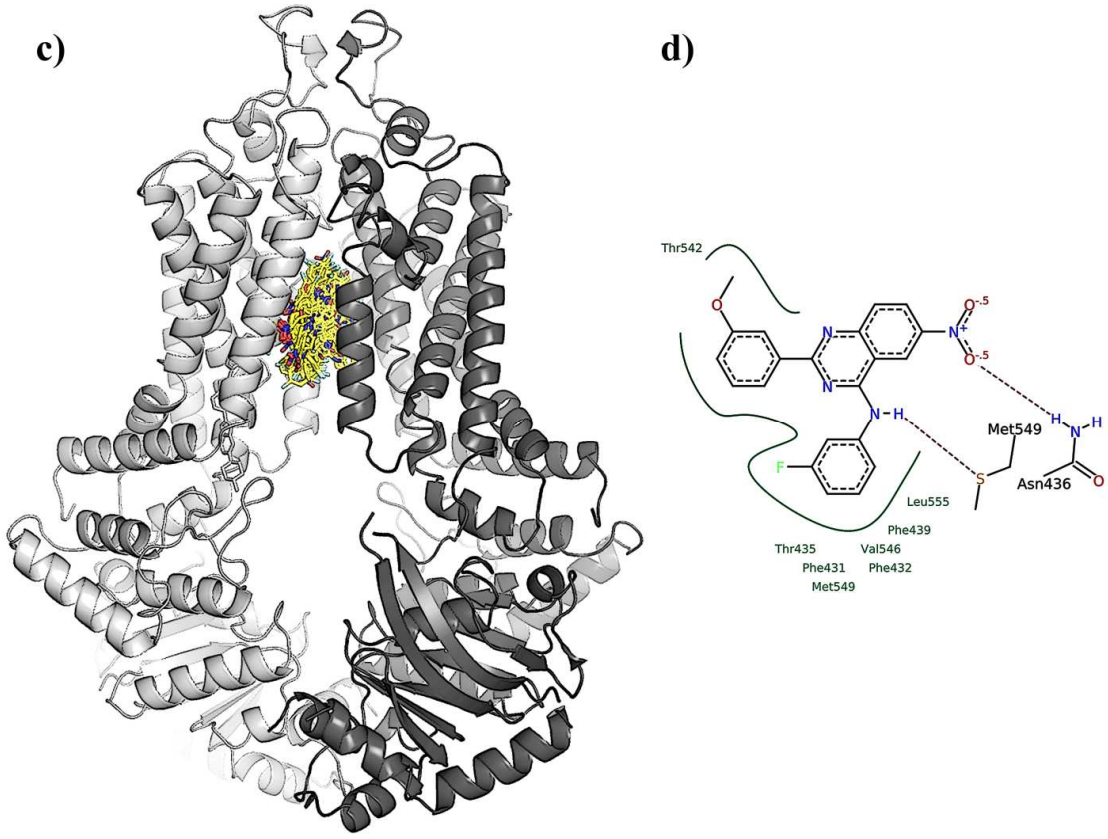

Figure 12. Putative binding poses of compound **31** and **41**. (a) The docked poses of **31** (green) observed in the cryo-EM structure of the human ABCG2 receptor (PDB ID: 6FFC) and (b) 2D interaction diagram. (c) The docked poses of **41** (yellow) observed in the cryo-EM structure of the human ABCG2 receptor and (d) 2D interaction diagram. The fluorine atoms are colored in cyan and for the remaining atoms see Figure 11 for color code

Table of Contents Graphic